Modelling of divertor plasma transport in stochastic magnetic boundary

M. Kobayashi

National Institute for Fusion Science, Oroshi-cho 322-6, Toki city 509-5292, Japan

In acknowledgement of the fruitful discussions and contributions from
Y. Feng, S. Morita, K. Ito, S. Masuzaki, T. Morisaki, N. Ezumi, S. Sakakibara, Y. Kikuchi, N. Ohyabu, T. Takizuka, S. Takamura, R. Burhenn, K.H. Finken, M. Lehnen, D. Reiter, S.S. Abdullaev, M.Z. Tokar, Ph. Ghendrih, T. Kobayashi, Y. Narushima, F. Sardei, the LHD experimental group

Role of SOL plasma in fusion reactor

Confinement region:
~10keV, 10^{20}m^{-3}, α-particle confinement/heating
control of pressure/current profile, 500MW fusion power, Q>10

Power through LCFS ⬇ ⬆ Impurity, fuel influx

Scrape-off layer:
1~few hundreds eV, 10^{20}~10^{21}m^{-3}, balance between // & $\perp$ transport, power removal with radiation, impurity transport (material migration), plasma flow distribution, interaction with neutrals

Power/particle flux ⬇ ⬆ Fuel recycling, impurity source

Material surface: divertor target, first wall
plasma neutralization, erosion, deposition, fuel retention, heat removal & fuel/He ash pumping

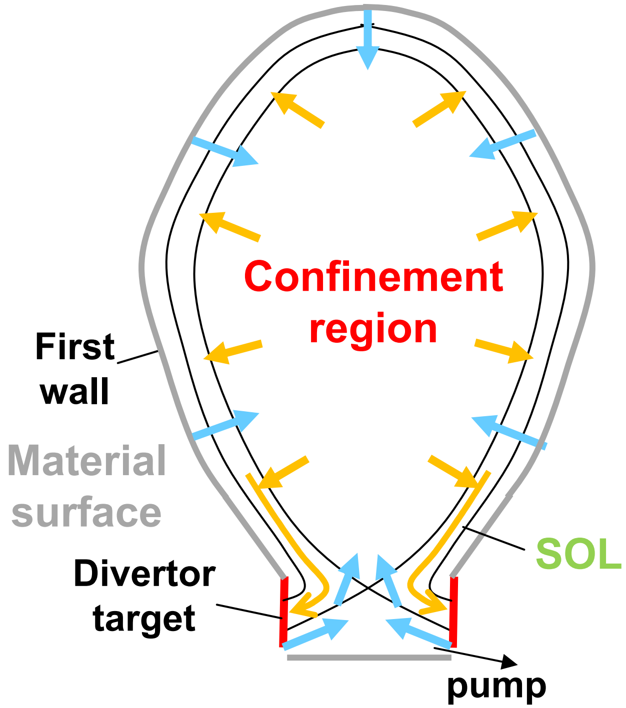

- ***Mitigation of power load on divertor plate***
- ***Reduction of Impurity influx to confinement region***
- ***High pumping efficiency of fuel, He ash***

Motivation

Stochastic field as a tool for controlling edge plasma

e.g. Ergodic divertor in TEXT, Tore Supra, TEXTOR-DED etc.
→ enhanced radial transport, edge radiation, impurity screening etc.

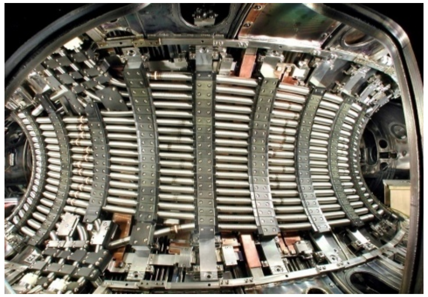

RMP for ELMs mitigation

RMP reduces pressure gradient, interacts with eigenmode structure of ELMs

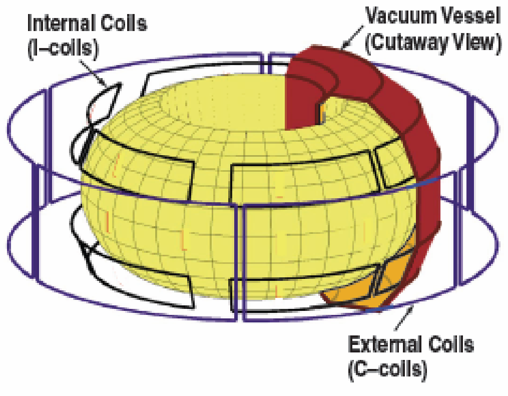

Intrinsic edge stochastization in Heliotron configuration

Understanding of plasma transport characteristics in stochastic field is inevitable for divertor optimization

Symmetry breaking by Resonant Magnetic Perturbation
2D axi-symmetric → 3D non-axi-symmetric

⇩

Controllability of edge plasma for divertor optimization

Study on plasma transport in stochastic field

Magnetic field structure

Island formaion, overlap (vacuum approximation)
← plasma response
(field amplification, rotational screening, neoclassical effect)

Measurements
← magnetic probe outside plasma, T_e profile

Ideal stochastization
← quasi-linear model, diffusive picture

Realistic field
← mixture of remnant islands, local ergodic field, laminar region

Transport analysis

Analytical formulae
(e.g. R-R model)

// & ⊥ transport interplay
(3D treatment)

Time averaged field
EMC3-EIRENE, E3D, FINDIF etc.

Fluctuating field
Electrostatic/electromagnetic turbulence (P. Beyer et al., DALF3) etc.

Contents of the talk

1. Formation of magnetic island and stochastic field
2. Realistic field structure in devices
3. Effects on transport (3D treatment)
   --- divertor plasma parameters
   --- SOL impurity transport
4. Summary
   --- further topics to be addressed

1. Formation of magnetic island and stochastic field

Formation of magnetic island : vacuum field

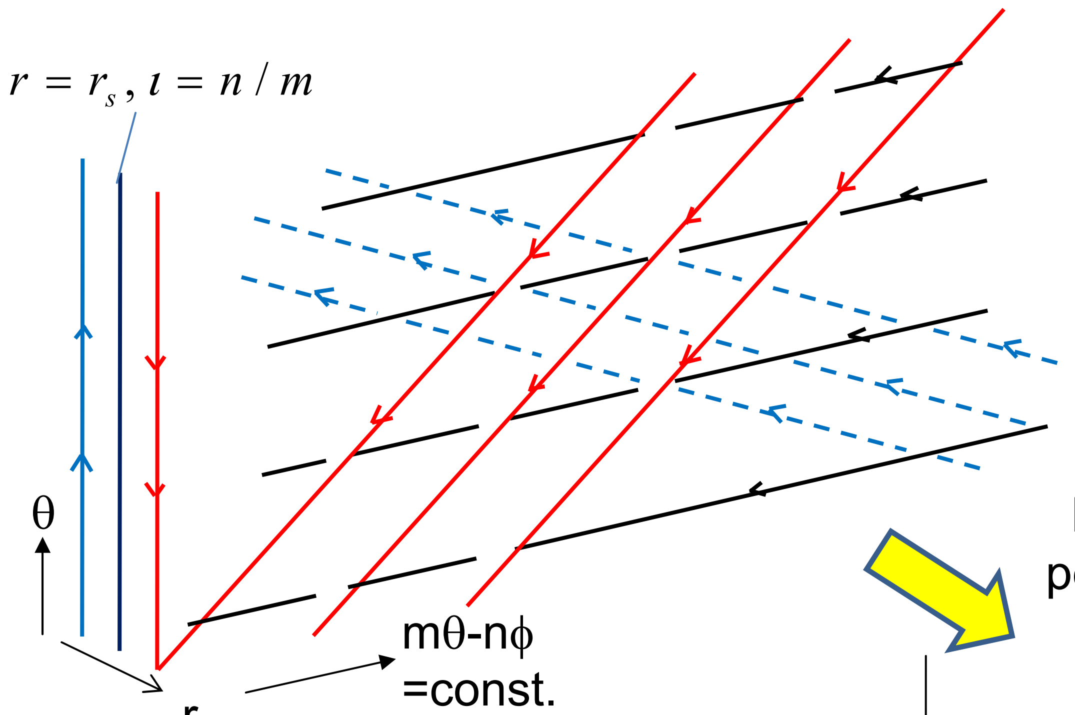

Projection onto resonant surface

Field lines change their helicity in radial direction because of magnetic shear.

$$\iota \equiv \frac{\Delta\theta}{2\pi} = \frac{1}{2\pi}\oint \frac{B_\theta R}{B_\phi r} d\phi = \frac{1}{q}$$

magnetic shear: $\frac{dq}{dr} = q'$

Resonant perturbation $\tilde{B}_r$

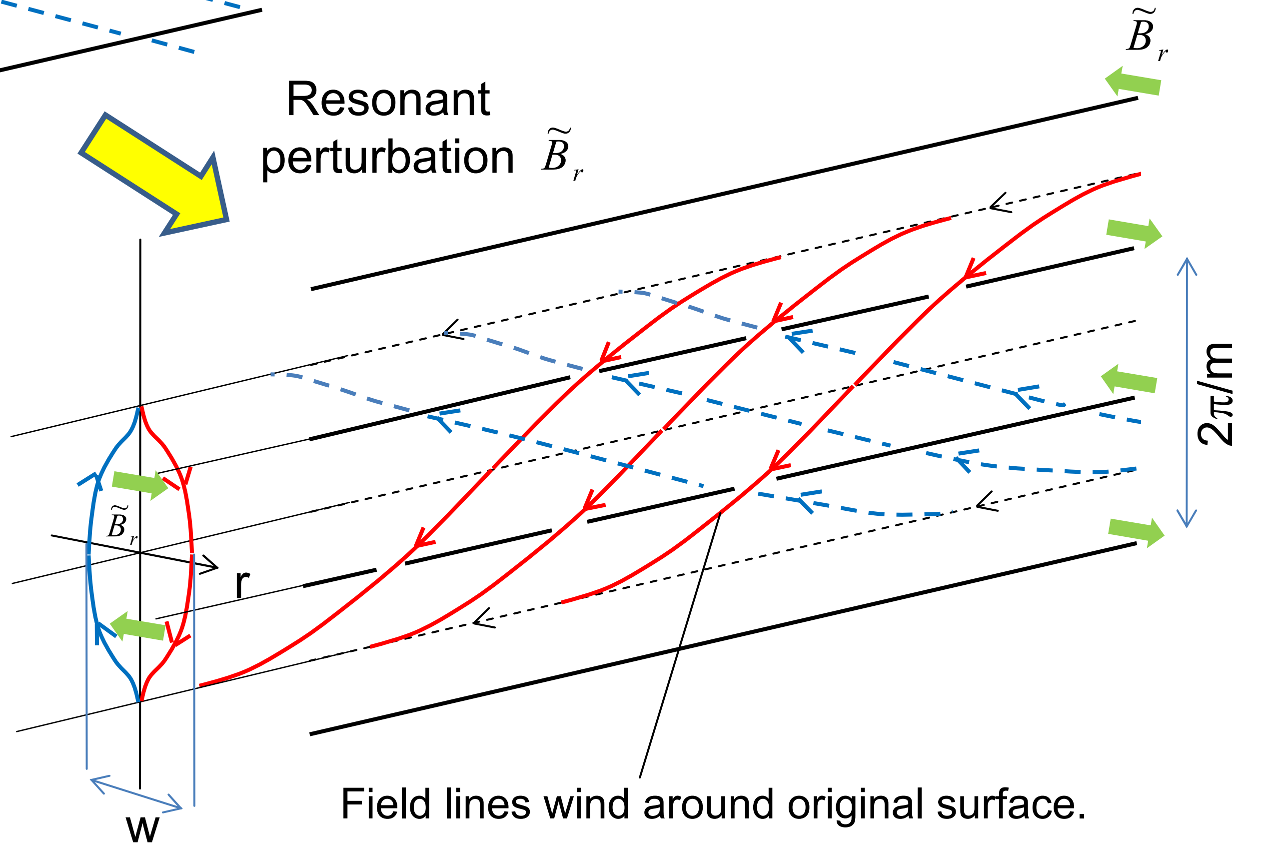

Radial component of RMP $\tilde{B}_r$ ( ) resonates with field line helicity (m,n).

$$\tilde{B}_r \propto \cos(m\theta - n\phi)$$

$$\tilde{B}_r / B_t = 10^{-5} \sim 10^{-4}$$

Island width

$$w = 4\sqrt{\frac{r_s q \tilde{B}_{rm,n}}{m q' B_\theta}} \sim \text{several cm}$$

Onset of stochastic instability by island overlapping: $\sigma_{Chir} > 1$

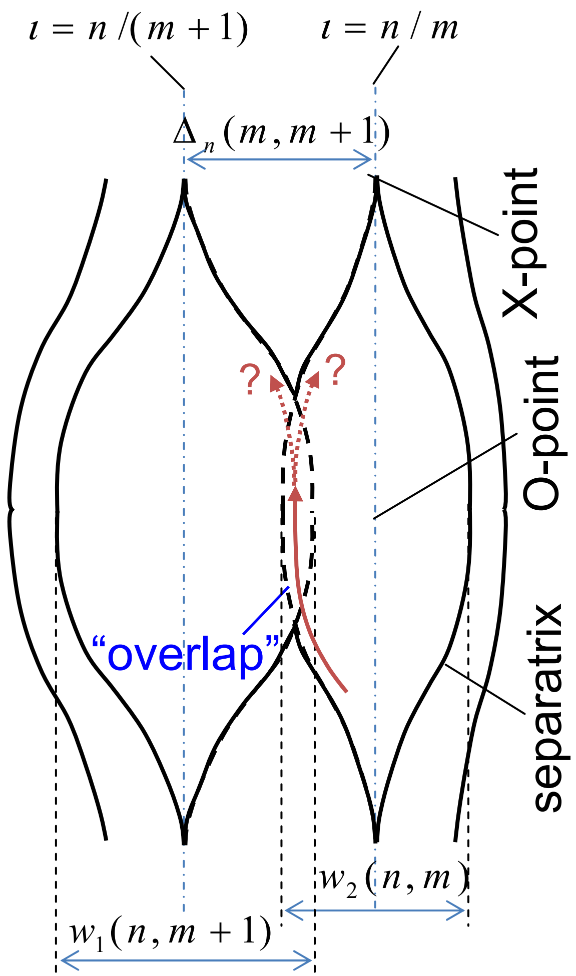

With increasing $\widetilde{B}_r$, island becomes large.

$$w \propto \sqrt{\widetilde{B}_{r\,m,n} / \iota'}$$

$$\sigma_{Chir}(n,m) = \frac{0.5(w_1 + w_2)}{\Delta_n(m, m+1)} > 1$$

Island "overlaps"

Field lines in overlap region share B field with neighboring island, and "forget" from which island come from.

Stochastic trajectories

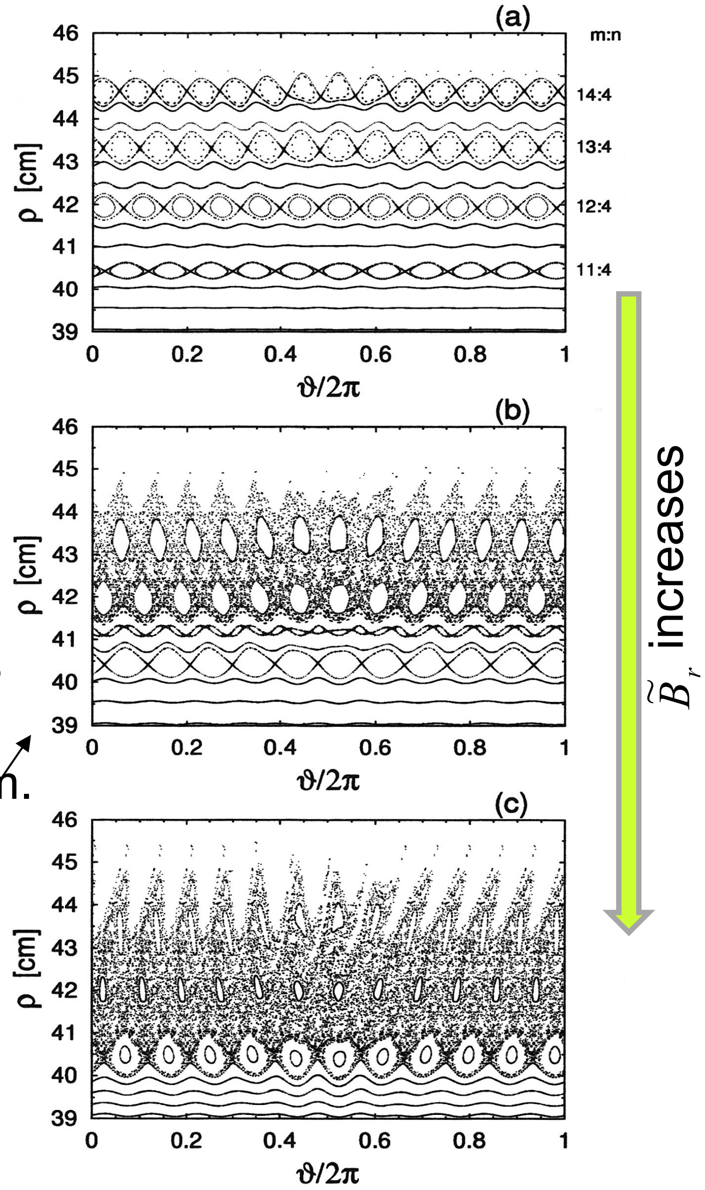

K.H. Finken et al., "The structure of magnetic field in the TEXTOR-DED"

Field line structure in stochastic magnetic boundary

Schematics of field line structure

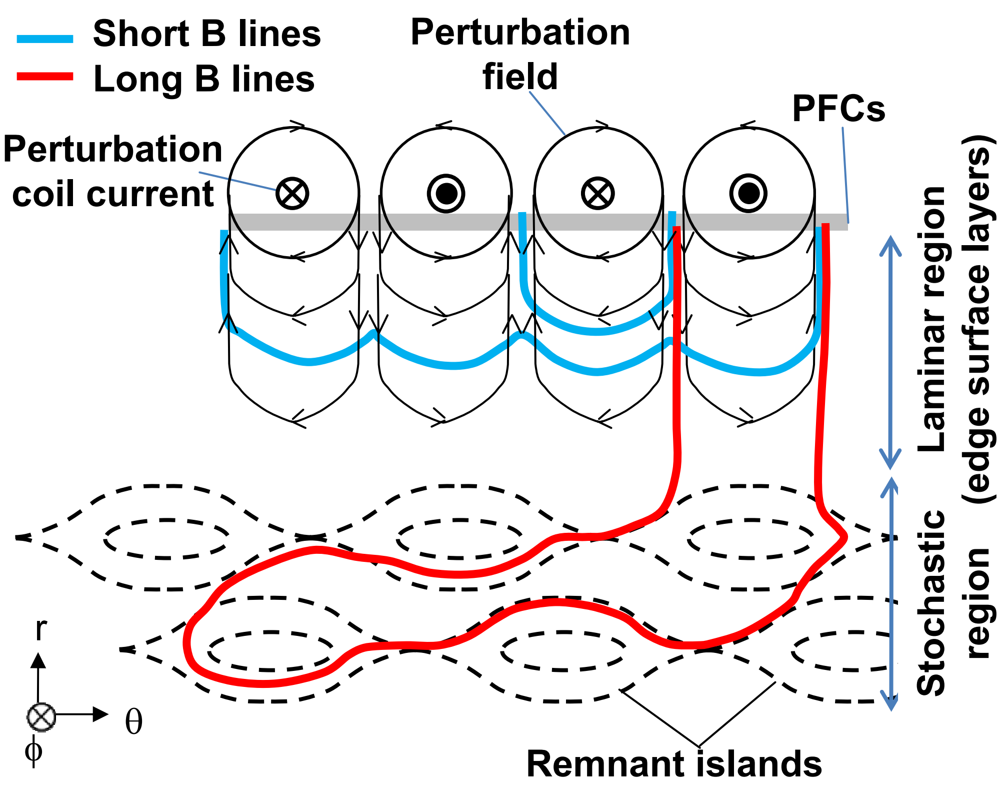

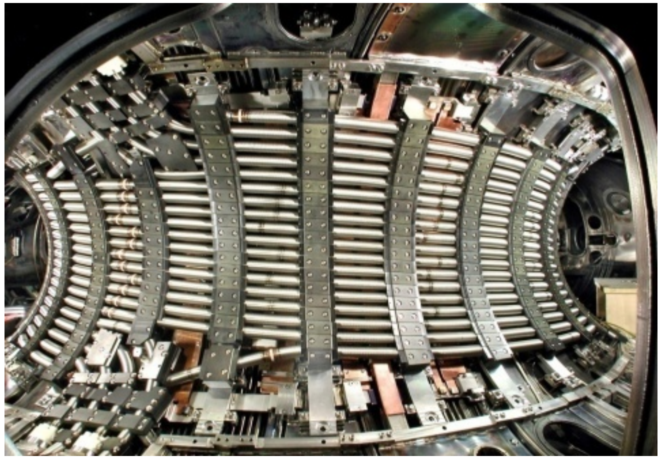

Connection length (L_C) distribution in TEXTOR-DED

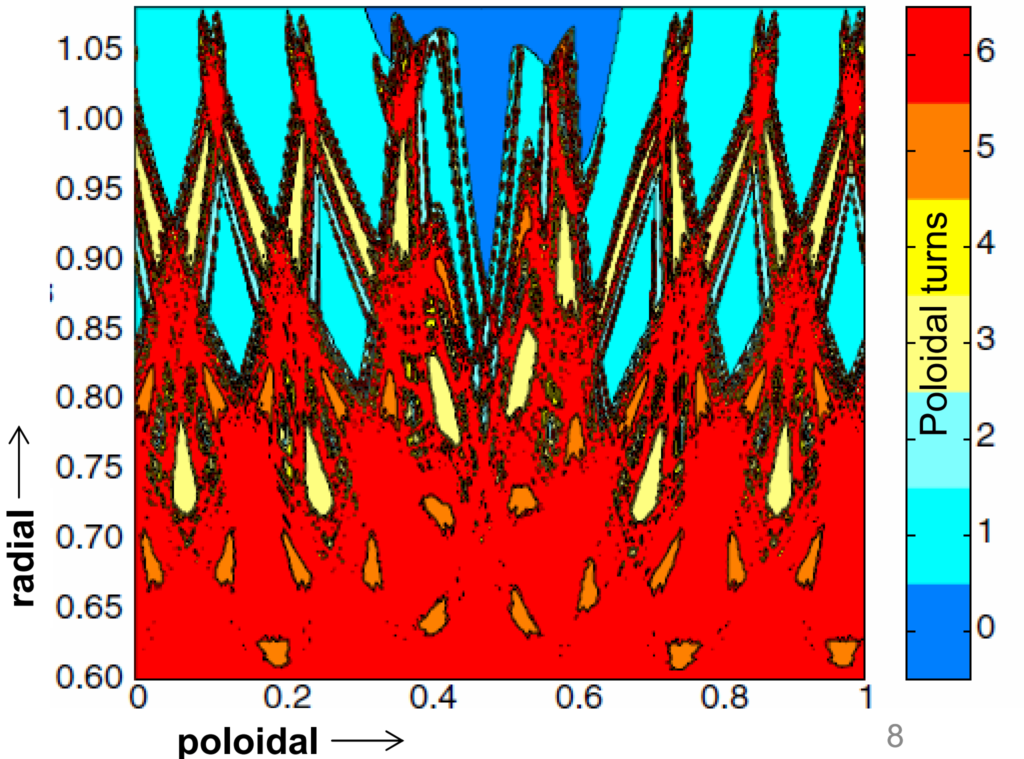

Laminar region (edge surface layers) ⇨ Short & long L_C coexist

Stochastic region ⇨ No clear separatrix, locally ergodic, remnant islands

K.H. Finken et al., PRL **98** (2007) 065001.

3. Effects on transport (3D treatment)

Magnetic field structure in LHD (Large Helical Device)

Connection length (L_C) distribution in poloidal cross section

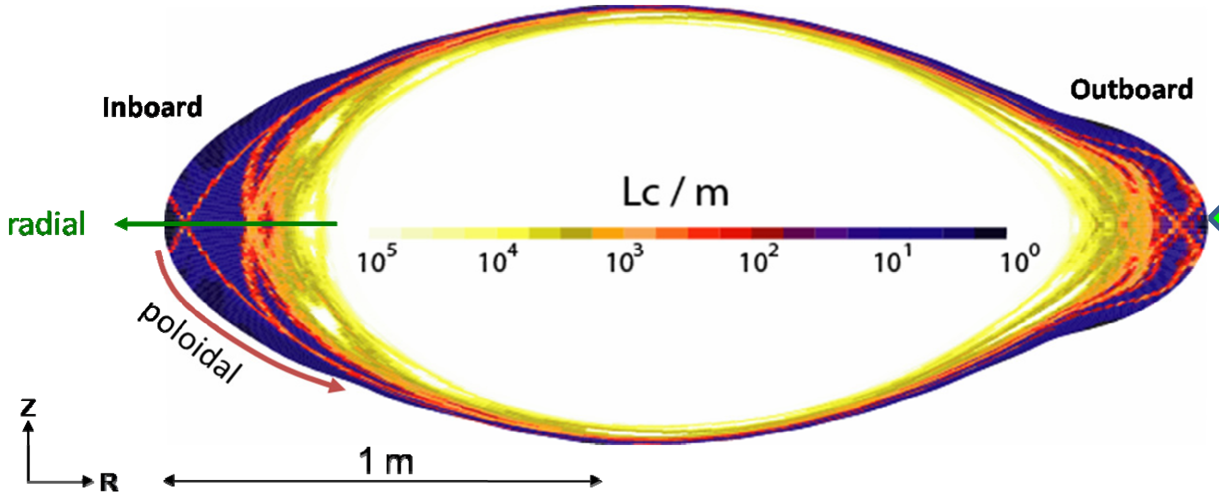

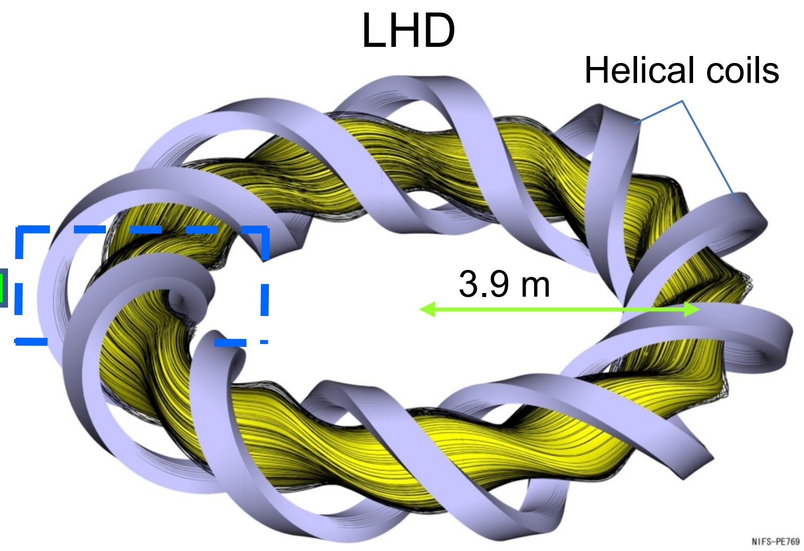

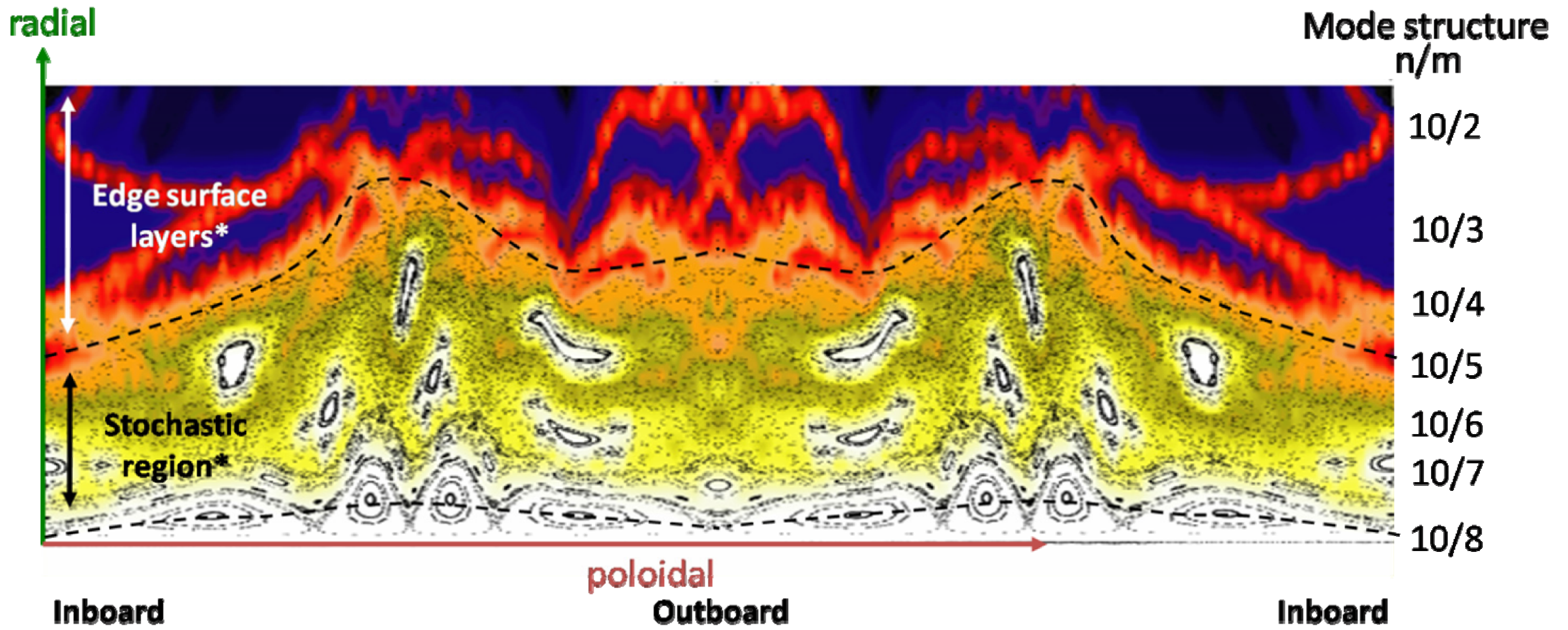

3D modelling of LHD edge region (EMC3-EIRENE)

Computational mesh, configuration and installations

- Core, CX-neutral transport, particle source
- SOL, EMC3 simulation domain
- Vacuum of plasma*

Physics model

- Standard fluid equations of mass, momentum, ion and electron energy
- Trace impurity fluid model (Carbon)
- Kinetic model for neutral gas (Eirene)

Boundary conditions

- Bohm condition at divertor plates
- Power entering the SOL
- Density on LCMS
- Sputtering coefficient

Cross-field transport coefficients

- $\chi_e=\chi_i$=3D roughly holds
- spatially constant (global transport)
- determined experimentally

Example of LHD helical divertor

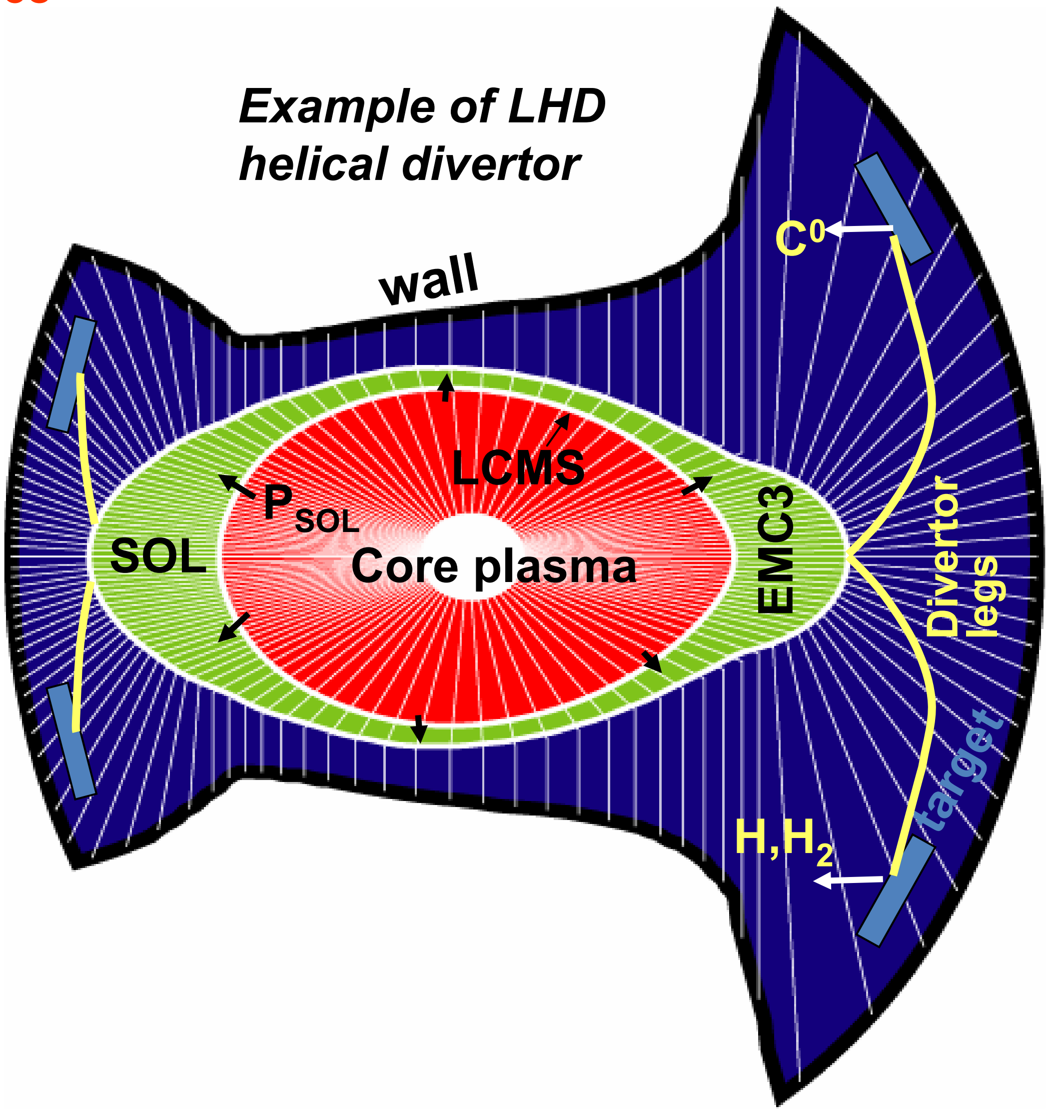

Model equations in EMC3-EIRENE

Background plasma (fluid):

$$\nabla\cdot\left(n_iV_{i\parallel}\boldsymbol{b}-D\boldsymbol{b}_\perp\boldsymbol{b}_\perp\cdot\nabla n_i\right)=S_p$$

$$\nabla\cdot\left(m_in_iV_{i\parallel}V_{i\parallel}\boldsymbol{b}-\eta_\parallel\boldsymbol{bb}\cdot\nabla V_{i\parallel}-m_iV_{i\parallel}D\boldsymbol{b}_\perp\boldsymbol{b}_\perp\cdot\nabla n_i-\eta_\perp\boldsymbol{b}_\perp\boldsymbol{b}_\perp\cdot\nabla V_{i\parallel}\right)=-\boldsymbol{b}\cdot\nabla p+S_m$$

$$\nabla\cdot\left(\tfrac{5}{2}n_eT_eV_{i\parallel}\boldsymbol{b}-\kappa_e\boldsymbol{bb}\cdot\nabla T_e-\tfrac{5}{2}T_eD\boldsymbol{b}_\perp\boldsymbol{b}_\perp\cdot\nabla n_e-\chi_en_e\boldsymbol{b}_\perp\boldsymbol{b}_\perp\cdot\nabla T_e\right)=-k\left(T_e-T_i\right)+S_{ee}+S_{imp}$$

$$\nabla\cdot\left(\tfrac{5}{2}n_iT_iV_{i\parallel}\boldsymbol{b}-\kappa_i\boldsymbol{bb}\cdot\nabla T_i-\tfrac{5}{2}T_iD\boldsymbol{b}_\perp\boldsymbol{b}_\perp\cdot\nabla n_i-\chi_in_i\boldsymbol{b}_\perp\boldsymbol{b}_\perp\cdot\nabla T_i\right)=+k\left(T_e-T_i\right)+S_{ei}$$

Impurities (fluid):

$$\nabla\cdot\left(n_I^zV_{I\parallel}^z\boldsymbol{b}-D_I^z\boldsymbol{b}_\perp\boldsymbol{b}_\perp\cdot\nabla n_I^z\right)=S_{z-1\to z}-S_{z\to z+1}+R_{z+1\to z}-R_{z\to z-1}$$

$$U_{Ii}^z\left(V_{I\parallel}^z-V_{i\parallel}\right)=-\boldsymbol{b}\cdot\nabla n_I^zT_I^z+n_I^zZeE_\parallel+n_I^zZ^2C_e\boldsymbol{b}\cdot\nabla T_e+n_I^zC_i\boldsymbol{b}\cdot\nabla T_i$$

$$\boldsymbol{b}\cdot\nabla n_eT_e+n_eeE_\parallel+n_eC_e\boldsymbol{b}\cdot\nabla T_e=0$$

$$T_I^z=T_i$$

Neutrals (kinetic):

Boltzmann equation (Eirene code)

Plasma-surface and neutral-surface interaction:

Particle and energy reflection, sputtering (Eirene code)

Field line aligned 3D grids

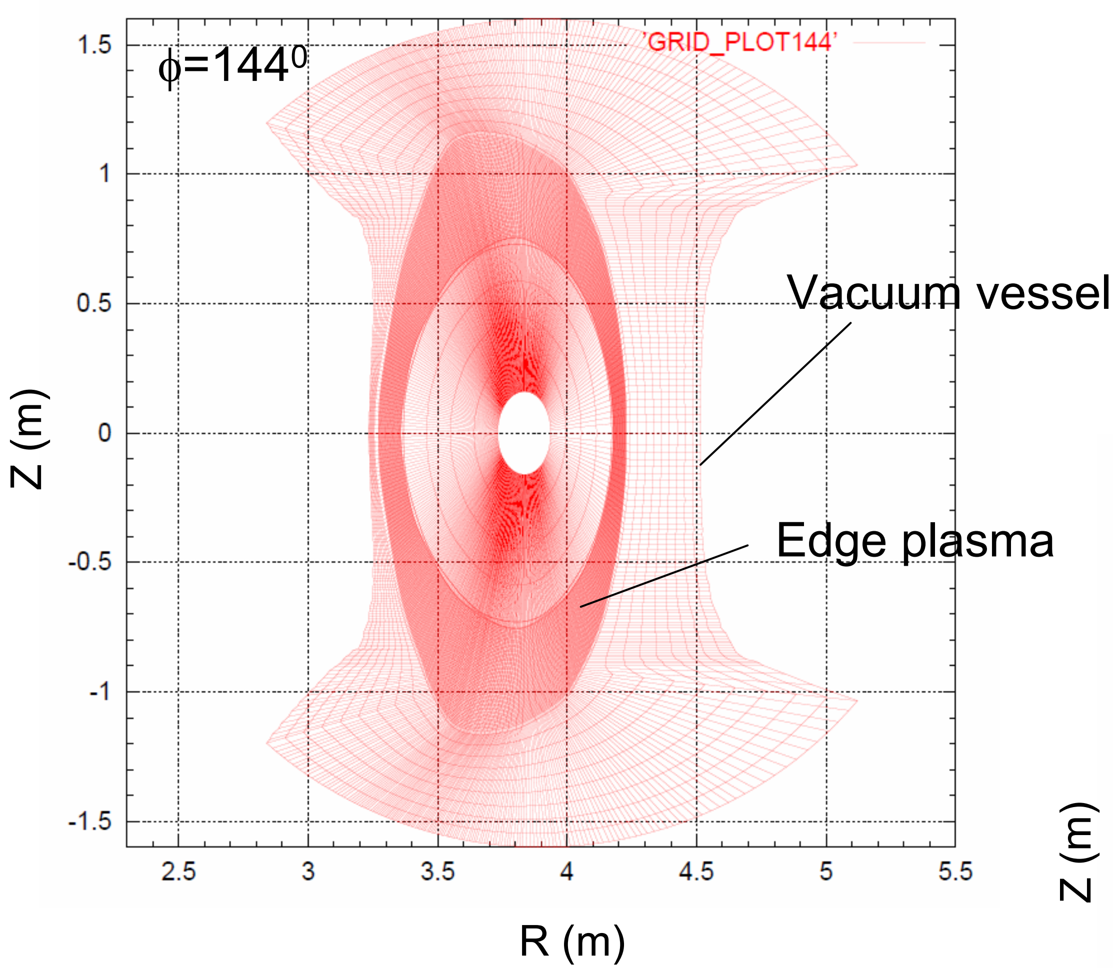

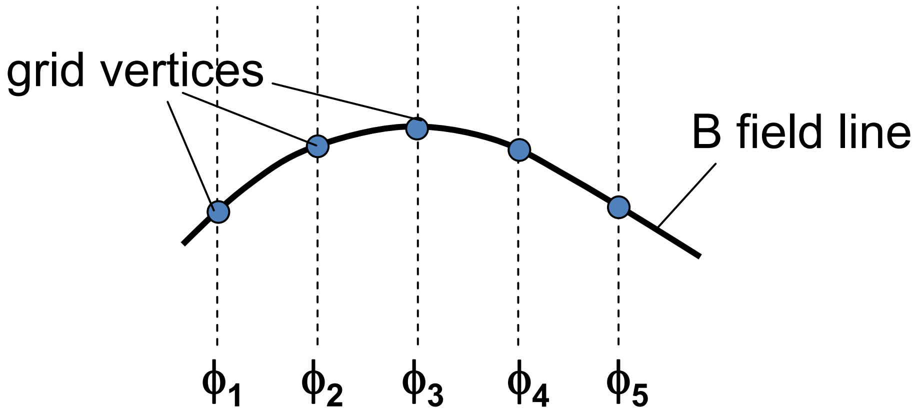

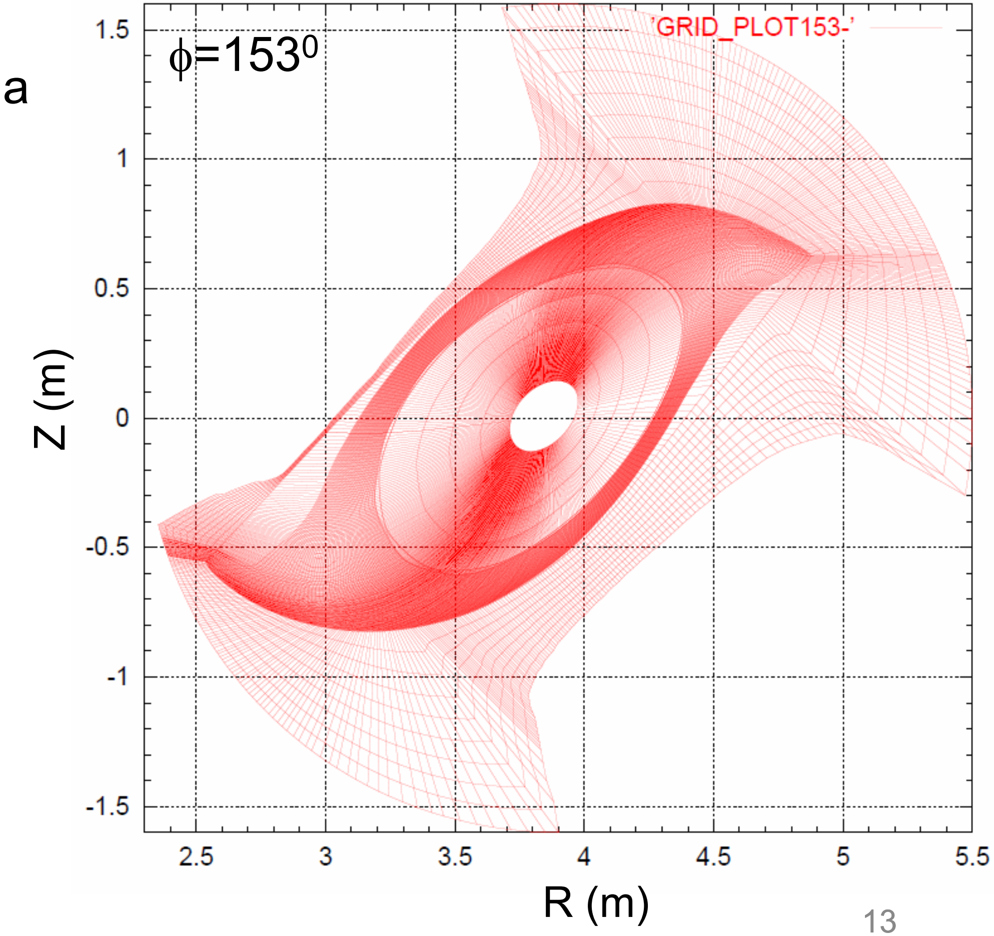

Jump step of Monte Carlo particle

Fokker-Planck form $$\nabla_{\|}\cdot[\mathbf{a}_{\|}f-\nabla_{\|}(b_{\|}f)]+\nabla_{\perp}\cdot[\mathbf{a}_{\perp}f-\nabla_{\perp}(b_{\perp}f)]=S,$$

<Coefficients for different f's>

f :	density n	velocity $\mathbf{V}_{\|}$	temperature $T_{i,e}$
$\mathbf{a}_{\|}$:	$\boldsymbol{V}_{\|}$	$m_i n\boldsymbol{V}_{\|}+\nabla_{\|}\eta_{\|}$	$\frac{5}{2}n\boldsymbol{V}_{\|}+\nabla_{\|}\kappa_{i,e}$
$b_{\|}$:	0	$\eta_{\|}$	$\kappa_{i,e}$
$\mathbf{a}_{\perp}$:	0	0	$(\chi_{i,e}-\frac{5}{2}D)\nabla_{\perp}n$
$b_{\perp}$:	D	$m_i nD$	$n\chi_{i,e}$
S :	S_p	$-\nabla_{\|}p+\boldsymbol{S_m}$	$\pm k(T_e-T_i)+S_{ei,ee}$

$$\Delta\mathbf{x}_{\|}=\sqrt{2b_{\|}\Delta t}\,\overrightarrow{\xi_{\|}}+\mathbf{a}_{\|}\Delta t,$$ **: $\mathbf{e}_3$**

$$\Delta\mathbf{x}_{\perp}=\sqrt{4b_{\perp}\Delta t}\,\overrightarrow{\xi_{\perp}}+\mathbf{a}_{\perp}\Delta t,$$ **: $\mathbf{e}_1$, $\mathbf{e}_2$**

($\overrightarrow{\xi_{\|}}$ $\overrightarrow{\xi_{\perp}}$: 1D and 2D random unit vectors)

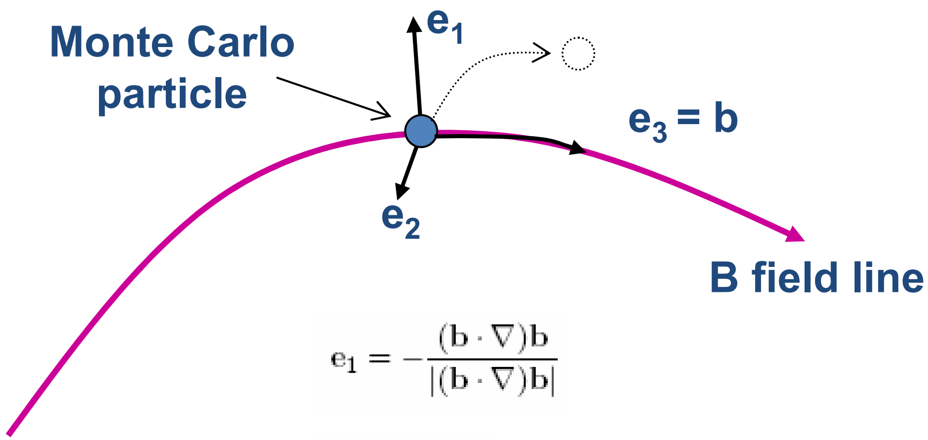

$$\mathbf{e}_1=-\frac{(\mathbf{b}\cdot\nabla)\mathbf{b}}{|(\mathbf{b}\cdot\nabla)\mathbf{b}|}$$

$$\mathbf{e}_2=\mathbf{b}\times\mathbf{e}_1$$

3. Effects on transport (3D treatment)
3.1 divertor plasma parameters

Role of pressure conservation along flux tubes on T_{div}, n_{div}

Divertor plasma parameter in ASDEX

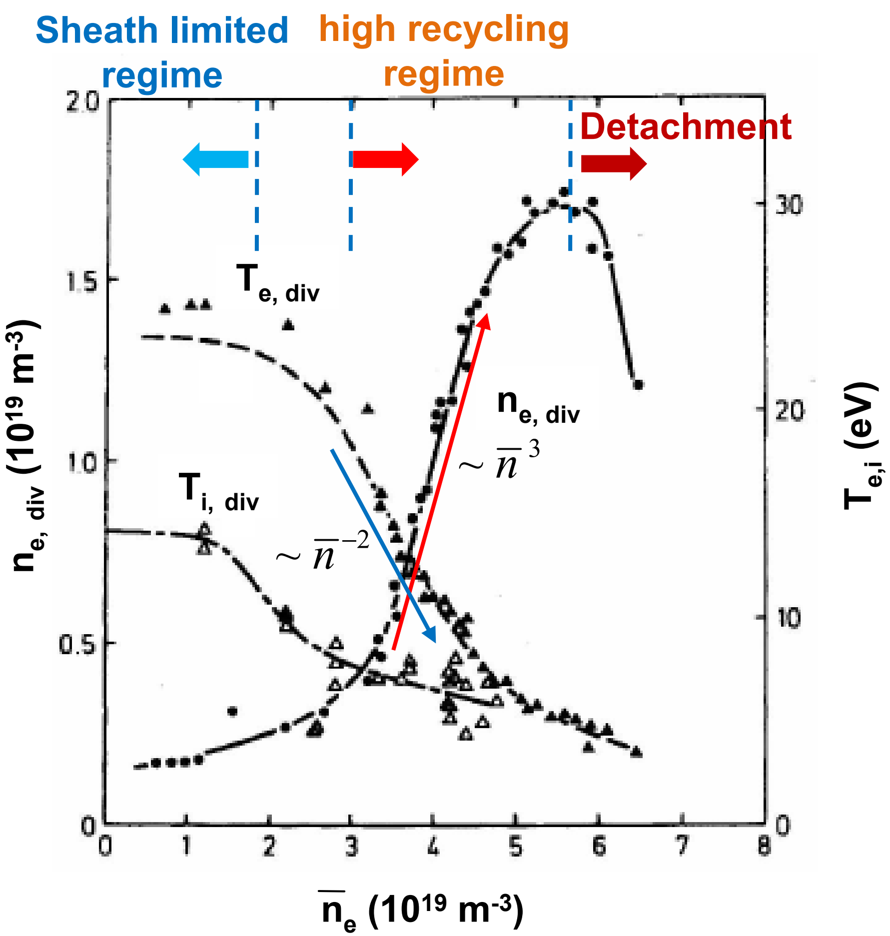

Y. Shimomura et al., NF **23** (1983) 869.

X-point divertor tokamaks

Pressure conservation along flux tube,

$$\nabla_{//}(nT + m_i n V_{//}^{2}) = 0$$

gives rise to sensitive divertor parameter dependence on upstream density :

High recycling regime (conduction limited regime)

$$n_{div} \propto n_{up}^{3} \qquad T_{div} \propto n_{up}^{-2}$$

The dependence is experimentally confirmed.

Stochastic boundary

The 3D flux tube geometry can introduce perpendicular terms → breaking down of the pressure conservation.

$$\nabla_{//}(nT + m_i n V_{//}^{2}) - \underline{\nabla_{\perp}(m_i V_{//} D_{\perp} \nabla_{\perp} n + \eta_{\perp} \nabla_{\perp} V_{//})} = 0$$

Parallel plasma flow is regulated by remnant island (mode) structure

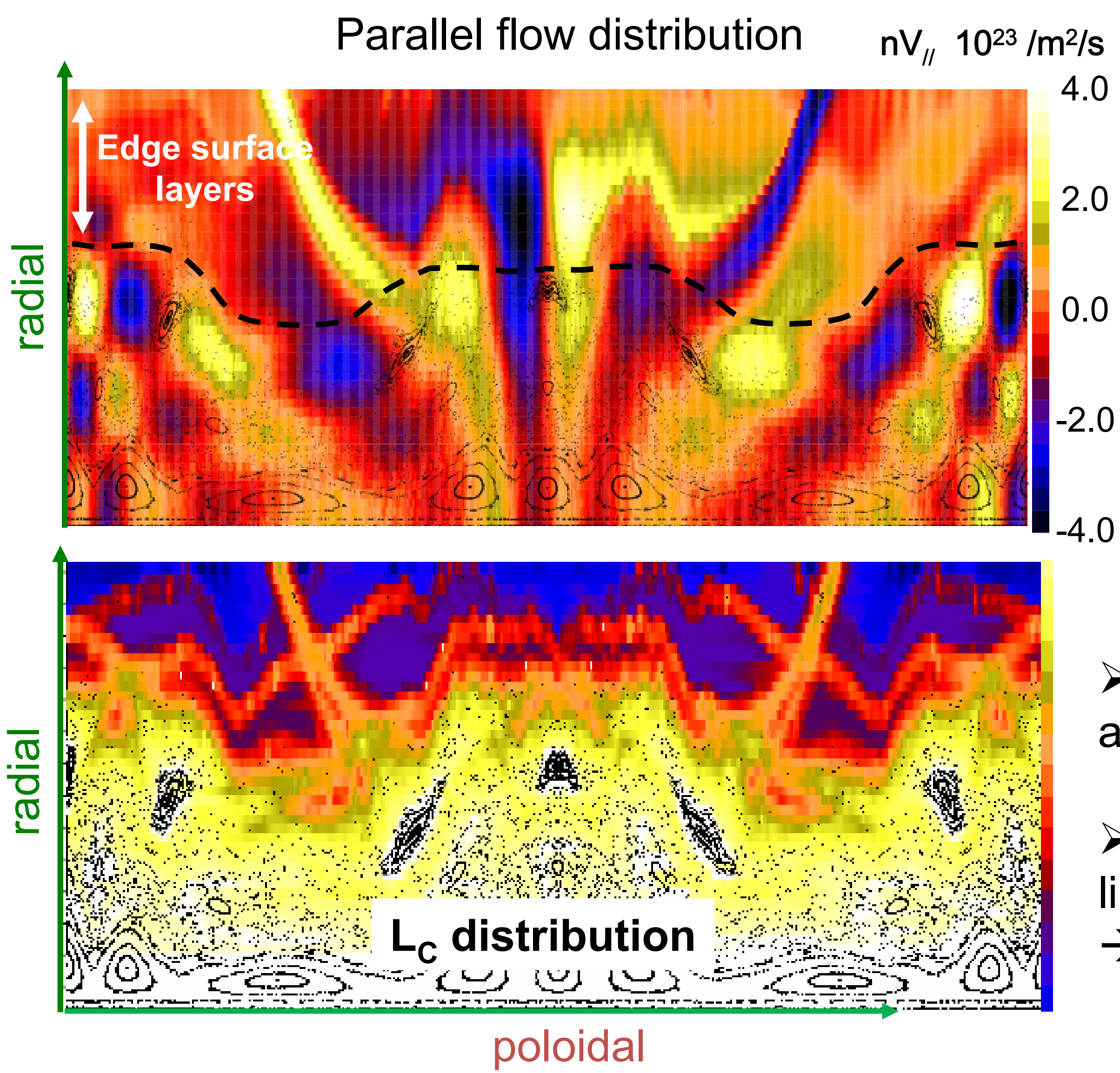

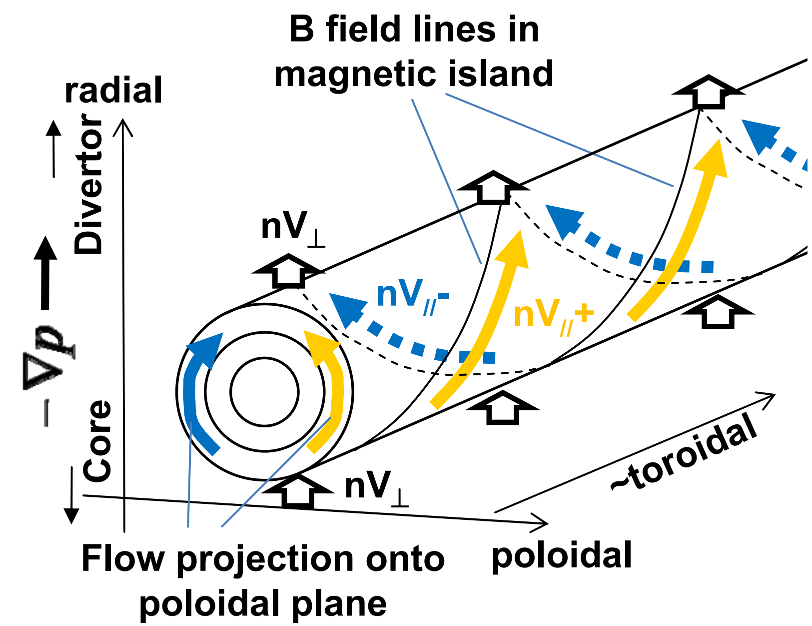

- The field line structure produces flow alternation.
- Short confinement time in open field lines leads to fast parallel flow
  →impact on impurity transport
  (discussed later)

Parallel plasma flow is regulated by remnant island (mode) structure

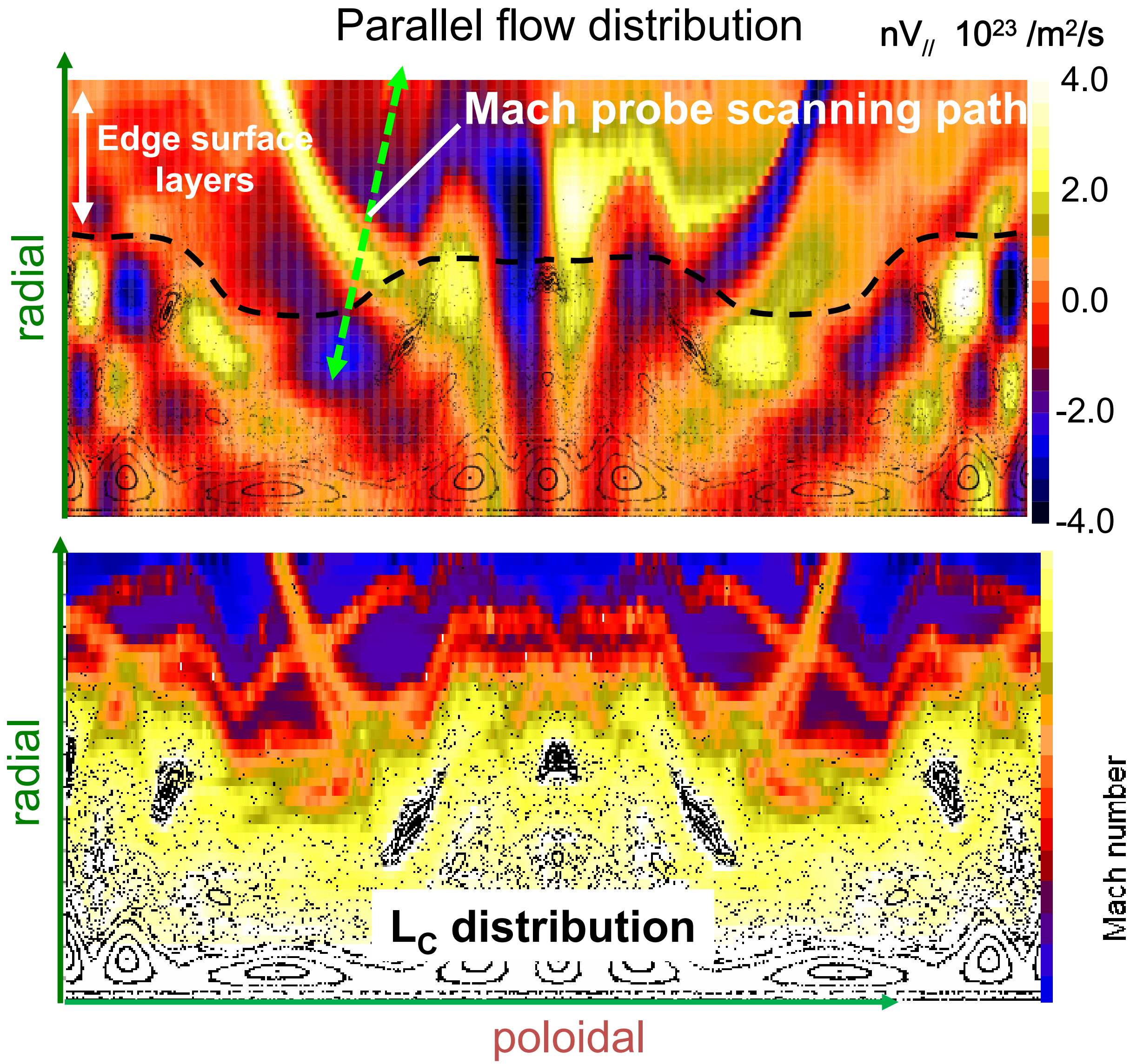

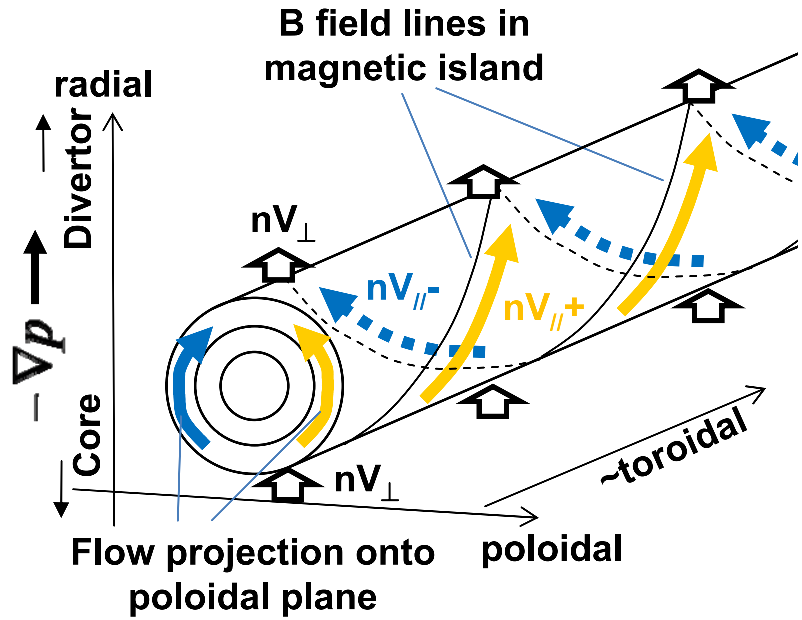

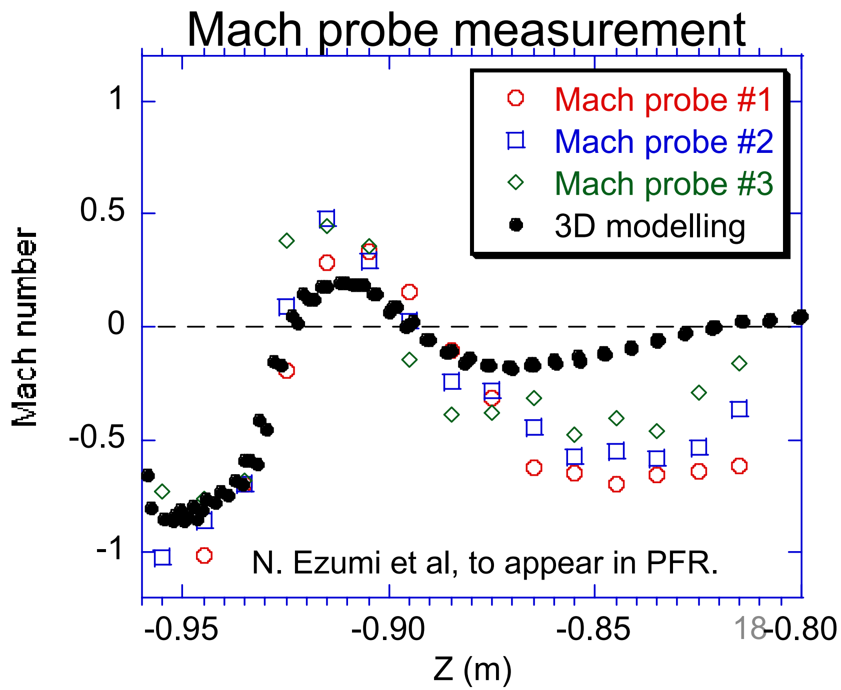

Parallel plasma flow is regulated by remnant island (mode) structure

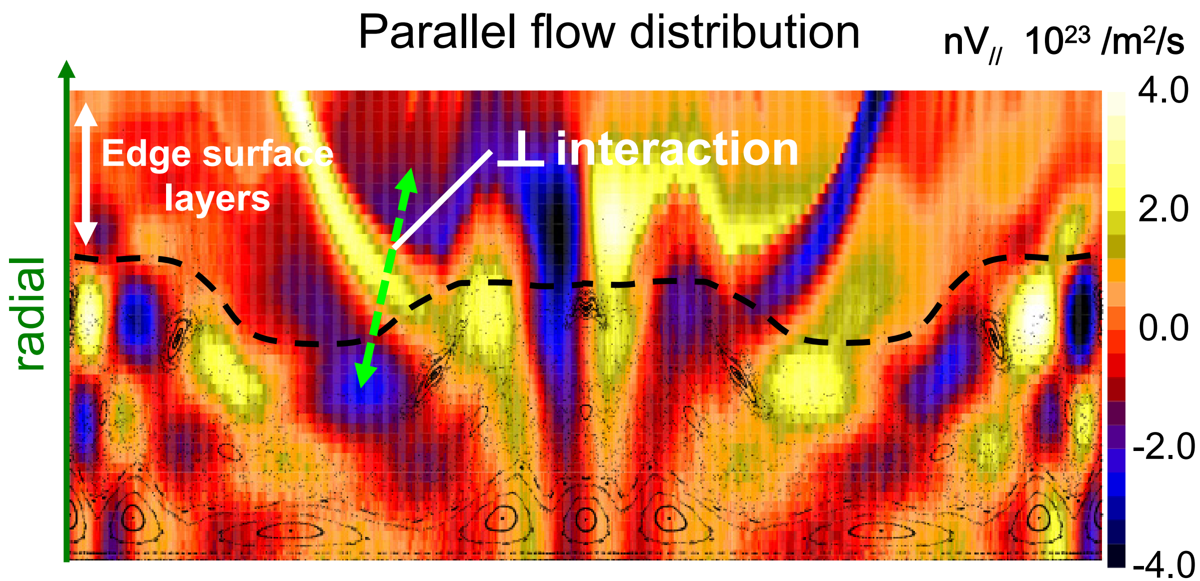

➢The flow shear → momentum loss of $V_{//}$ via ⊥ interaction

$$\nabla_{\perp}(m_i V_{//} D_{\perp} \nabla_{\perp} n + \eta_{\perp} \nabla_{\perp} V_{//})$$

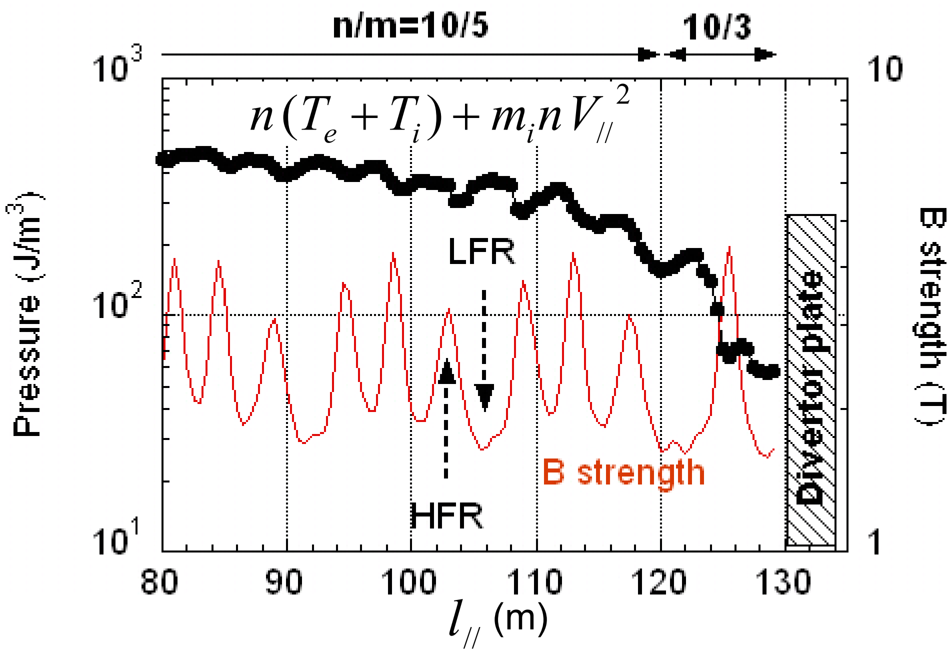

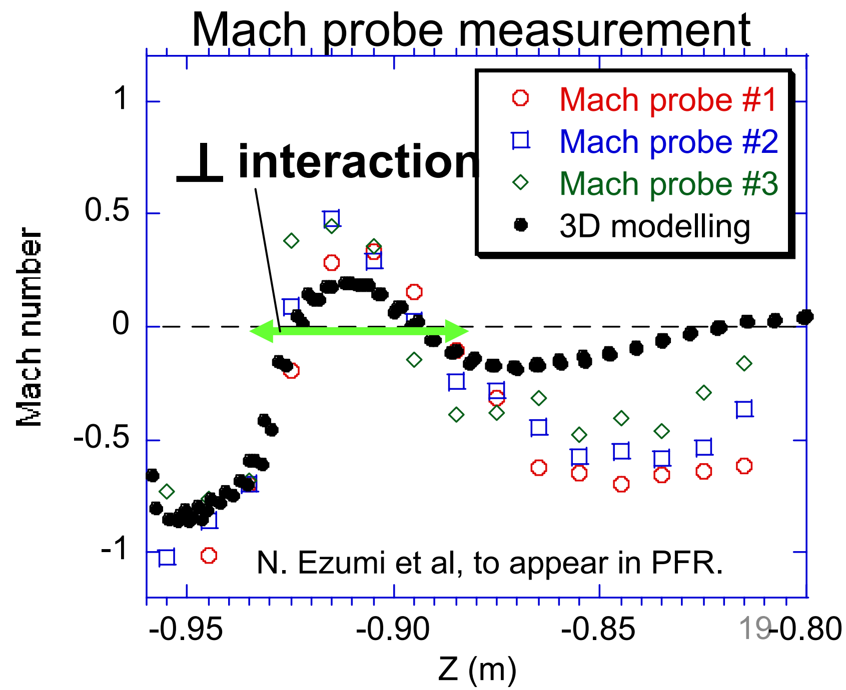

Two point model with momentum loss in perpendicular direction

$$T_d \propto n_u^{-2}(1+f_m)^2,$$
$$n_d \propto n_u^{3}(1+f_m)^{-3}$$

$$f_m = \frac{D}{2c_{sd}}\frac{1}{n_d c_{sd}}\int_d^u \nabla_\perp^2 n V_{//} dl \approx \frac{f_{m0}}{T_d^{0.5}} \propto \frac{l_{//}}{T_d^{0.5}\delta_m^2}$$

(Assumed D=const.)

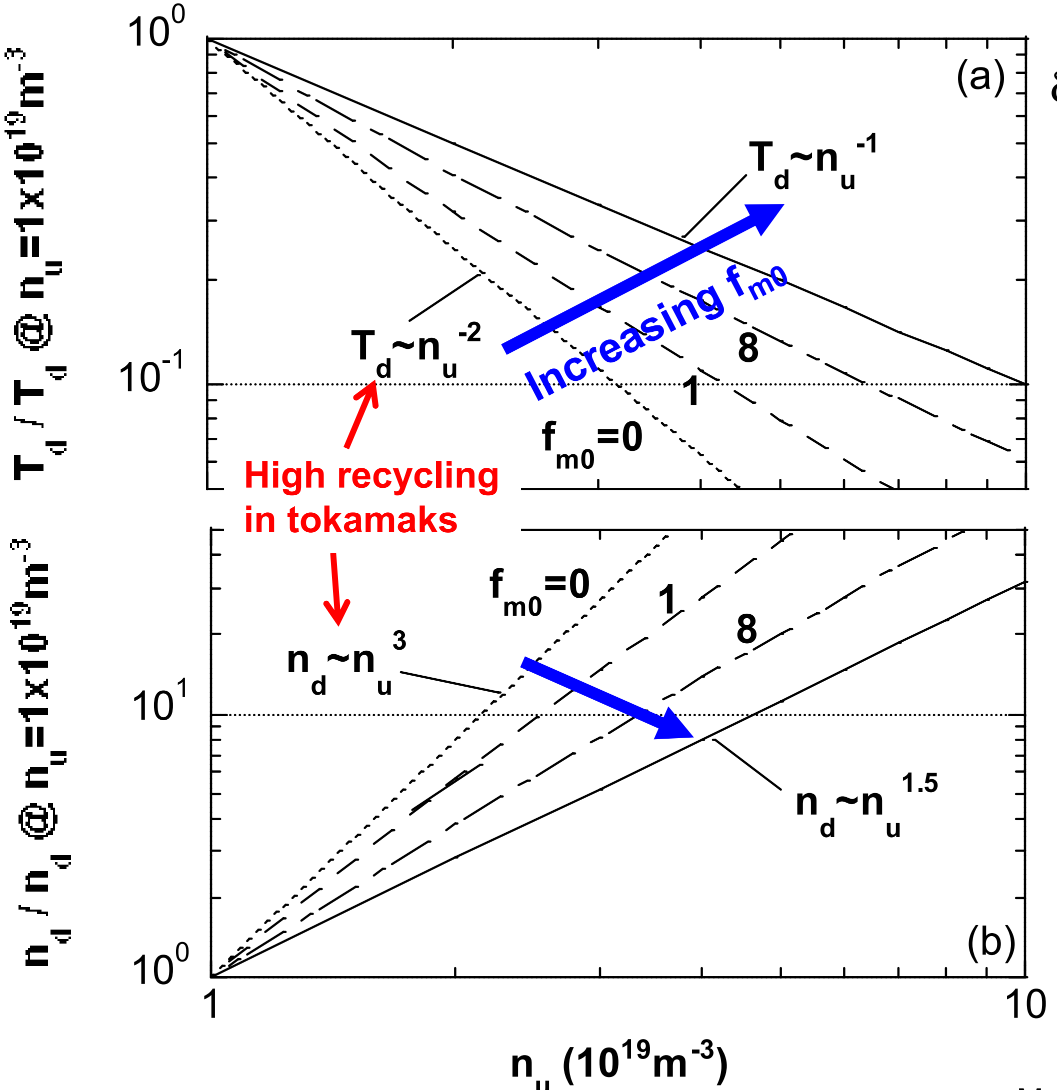

δ_m: ⊥ characteristic length of the flow alternation

$l_{//}$: distance along field line

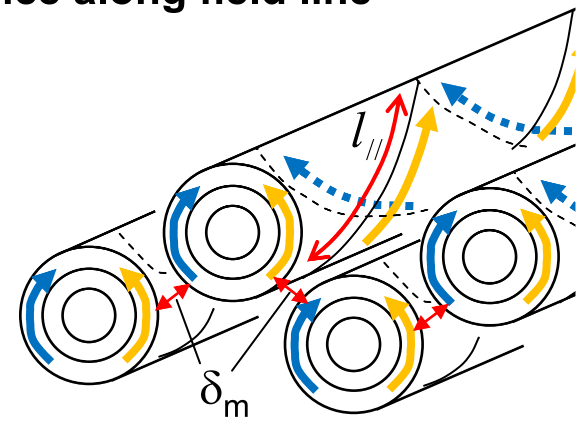

- $f_{m0}=0$ → high recycling in tokamaks

$$T_d \propto n_u^{-2} \qquad n_d \propto n_u^{3}$$

- Strong flux tube deformation
  → large f_{m0}, large momentum loss
  → modest dependence on n_u

$f_{m0}>>1$ → $T_d \propto n_u^{-1} \qquad n_d \propto n_u^{1.5}$

M. Kobayashi et al, to appear in JPFR (in Japanese), submitted to FS&T.

Divertor probe measurements confirm absence of high recycling regime prior to detachment

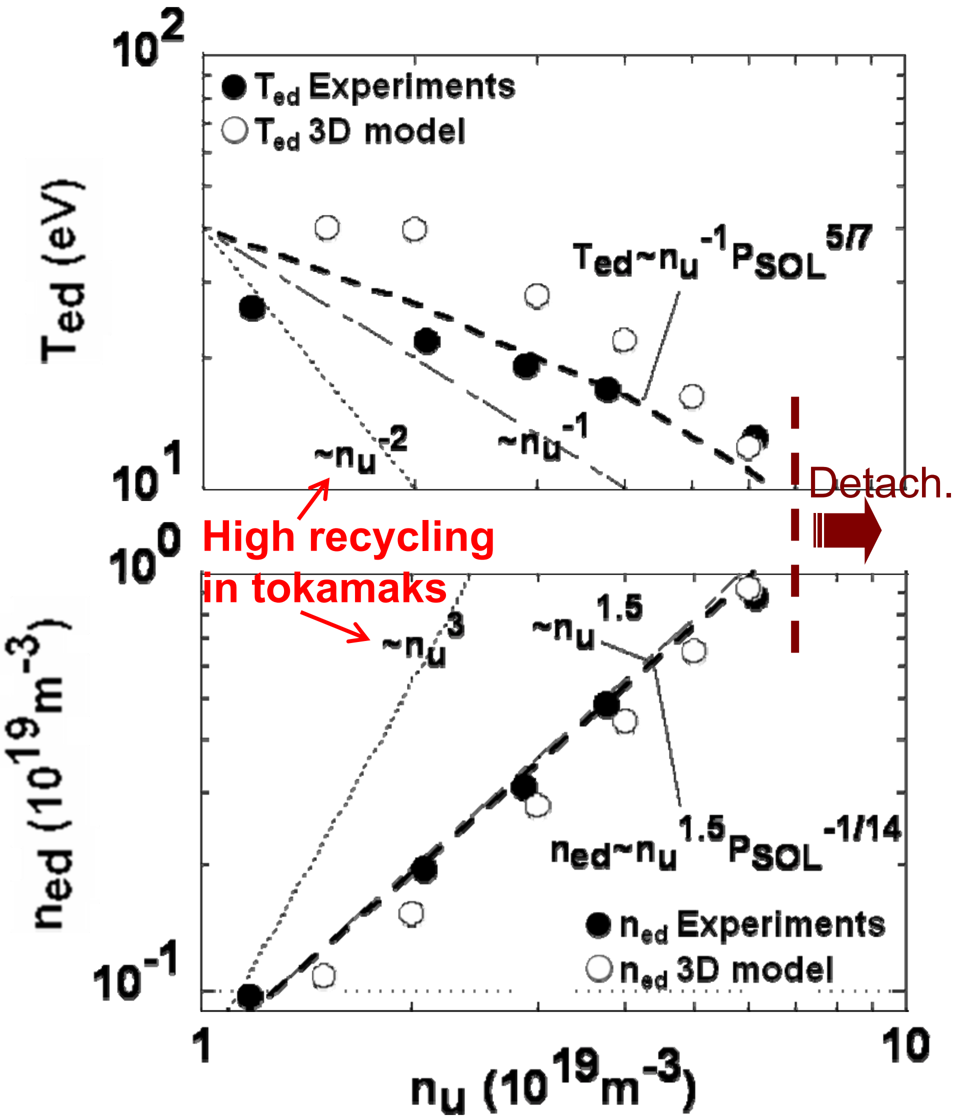

$$T_d \propto P_{SOL}{}^{10/7} n_u{}^{-2} (1+f_m)^2,$$

$$n_d \propto P_{SOL}{}^{-8/7} n_u{}^{3} (1+f_m)^{-3}$$

- Moderate dependence of T_{ed} & n_{ed} on n_u (T>10eV ← no significant CX loss, $\nu_{SOL}{}^*=L_C/mfp>10$)
- n_{ed} never exceeds upstream density

- Both 3D modellings & the two point model (with P_{SOL} variation due to NBI heating included) reproduce the experimental results.
  → effect of momentum loss via ⊥ interaction

M. Kobayashi et al, to appear in JPFR (in Japanese), submitted to FS&T.

Momentum loss via friction between counter flows in W7-AS/X

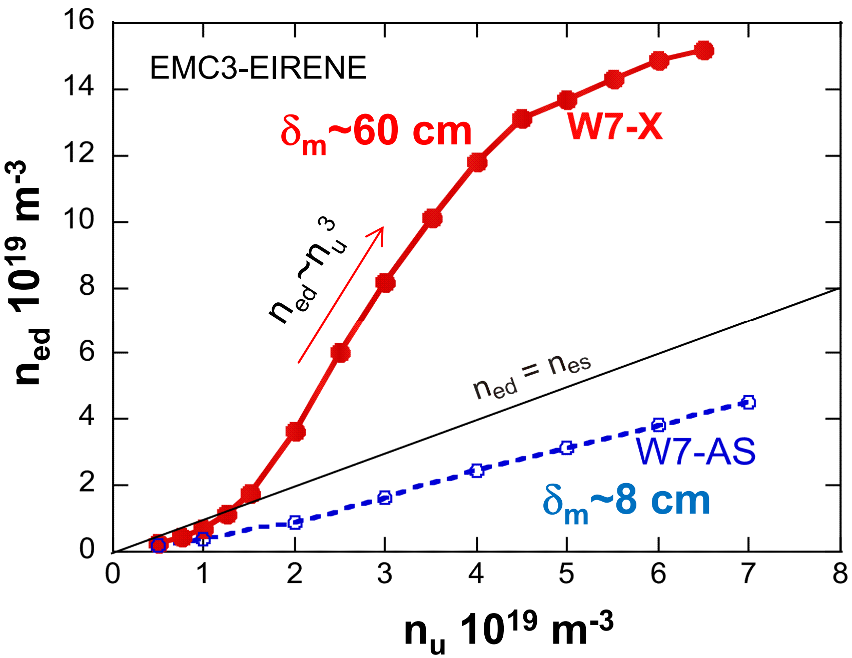

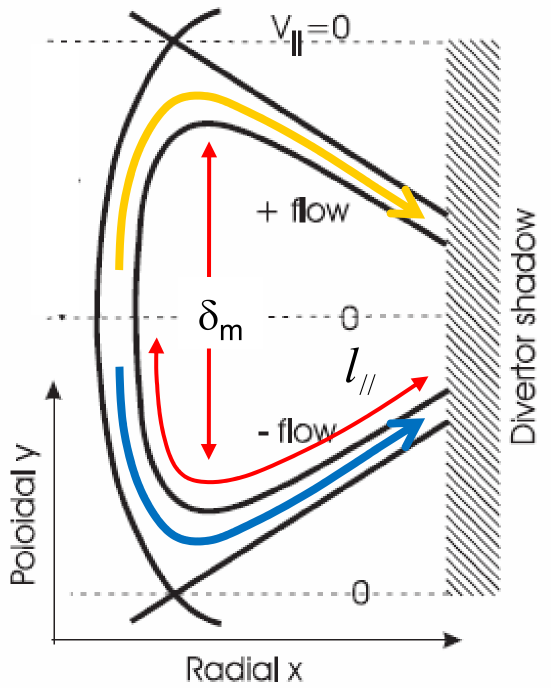

Y. Feng et al., NF **46** (2006) 807, Y. Feng et al., submitted to NF.

$$f_m \propto \frac{l_{//}}{T_d^{0.5}\,\delta_m^{2}}$$

W7-AS: $l_{//}$ ~100 m, δ_m~8 cm
W7-X: $l_{//}$ ~180 m, δ_m~60 cm

$\Rightarrow$ $f_{m,W7-AS} >> f_{m,W7-X}$

Field line geometry near divertor, $l_{//}, \delta_m$, provides controllability of divertor regime.

Summary of 3.1 Divertor plasma parameters

1. $nV_{//}$ in stochastic boundary → alternating flow regulated by remnant islands
2. n_{div} & T_{div} in stochastic boundary of LHD show modest sensitivity to n_{up}, in contrast to the high recycling regime in tokamaks.
3. Breakdown of parallel pressure conservation via perpendicular frictional interaction of the counter flows.
4. The degree of momentum loss can be described as $f_m \propto \dfrac{l_{//}}{T_d^{\,0.5}\,\delta_m^{\,2}}$.
5. The analysis in W7-AS, X
   → controllability of divertor regime: $n_d \propto n_u^{\,3}$ ←→ $n_d \propto n_u^{\,1\sim1.5}$
6. For future devices, $l_{//}, \delta_m$ should be optimized for control of divertor plasma with stochastic magnetic field.

3. Effects on transport (3D treatment)

3.2 SOL impurity transport

3D impurity transport model : EMC3-EIRENE (fluid approximation)

Momentum : // - Classical force balance

$$m_z \frac{\partial V_{z//}}{\partial t} = \underbrace{-\frac{1}{n_z}\frac{\partial T_i n_z}{\partial s}}_{\text{Impurity pressure gradient force}} + \underbrace{\boxed{m_z \frac{V_{i//} - V_{z//}}{\tau_s}}}_{\text{Friction}} + \overbrace{ZeE_{//}}^{\text{Electric field}} + \underbrace{0.71 Z^2 \frac{\partial T_e}{\partial s} + \boxed{2.6 Z^2 \frac{\partial T_i}{\partial s}}}_{\text{electron \& ion temperature gradient force (thermal force)}} + \ldots.$$

$\tau_s \searrow$ ⇨ friction $\nearrow$ $\frac{\partial T}{\partial s} \nearrow$ ⇨ $\pm V_{Z//}$?

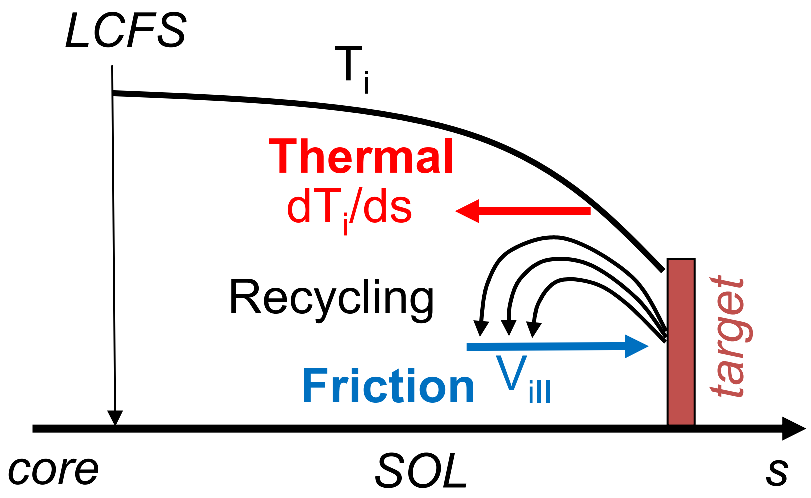

Mass : ⊥ - Diffusion with anomalous coefficient

$$\vec{\nabla} \cdot \left(n_z V_{z//} \vec{b} - D_z \vec{b}_\perp \vec{b}_\perp \cdot \vec{\nabla} n_z \right)$$
$$= S_{z-1 \to z} n_{z-1} - S_{z \to z+1} n_z + R_{z+1 \to z} n_{z+1} - R_{z \to z-1} n_z$$

D_z is set to be the same value of bulk plasma that is deduced from experiments.

From thermal-force to friction-dominated impurity transport

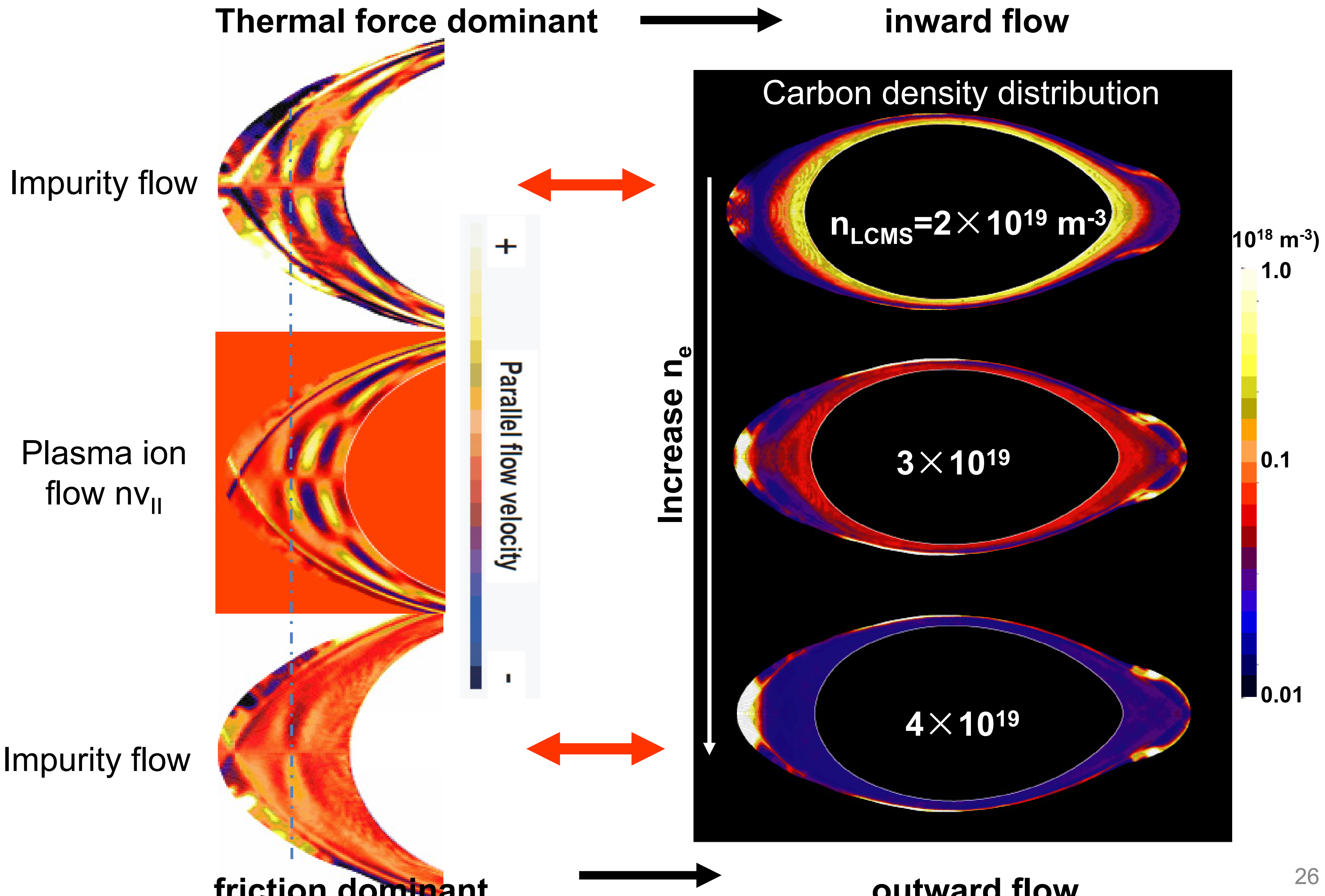

Carbon density profiles by 3D model show impurity retention at high density

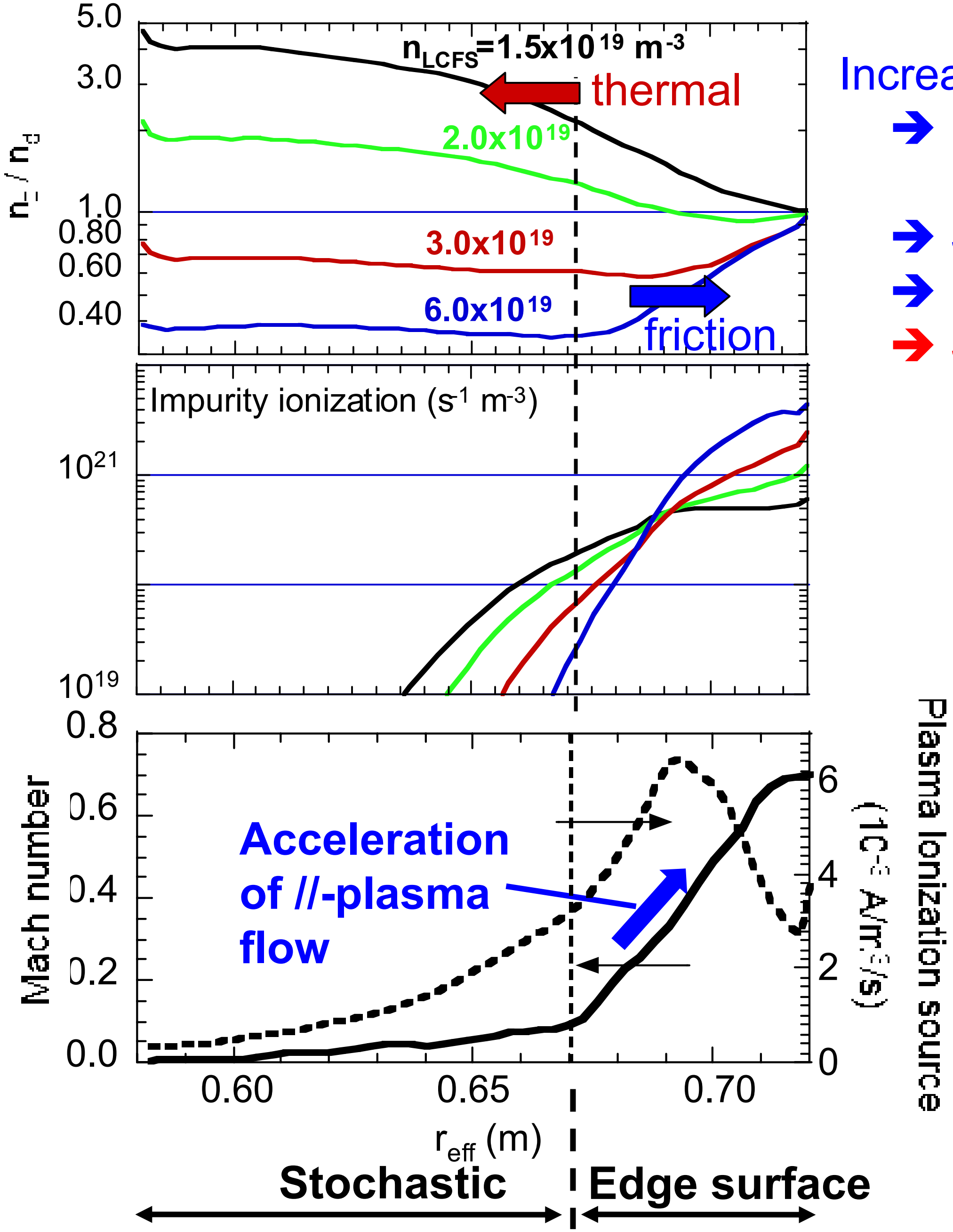

Increasing density

- ➔ Enhances friction force in edge surface layer with flow acceleration by short flux tubes
- ➔ Stops carbon penetration in edge surface layers
- ➔ Feels more friction
- ➔ Suppresses thermal force in stochastic region

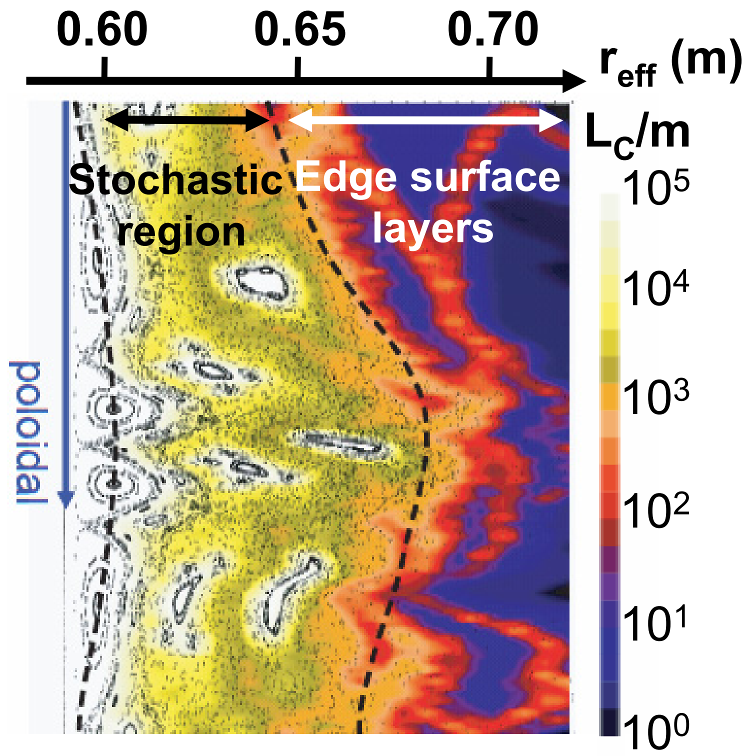

ITER International Summer School 2009, 22-26 June 2009, Aix en Provence, France

3D code predicts that energy transport follows the remnant island structure ➔ strong modulation of Te distribution

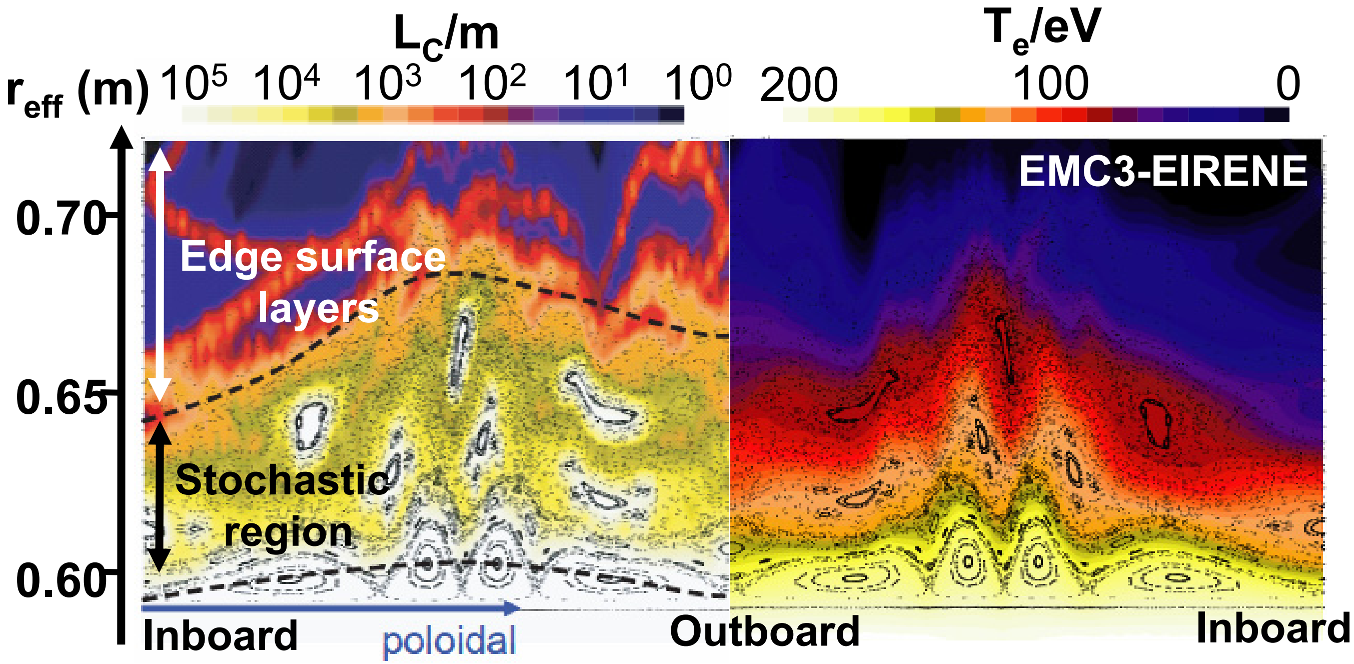

Clear mode structure is observed in Te profiles obtained by Thomson scattering system
→ in good agreement with the code result.

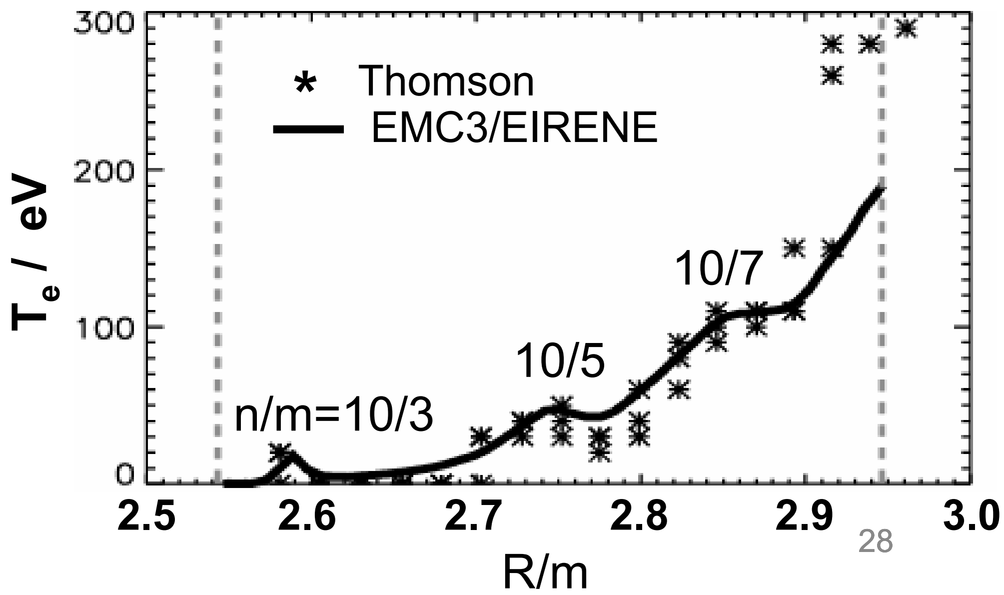

Key role of remnant islands on impurity transport

$$q_r = \underbrace{-n\chi_\perp \frac{\partial T_i}{\partial r}}_{\perp} \underbrace{-\vec{b}\cdot\vec{r}\,\kappa_{i0} T_i^{2.5} \nabla_{//} T_i}_{//}$$

$$\nabla_{//} T_i = -\frac{q_r \Theta}{n\chi_\perp + \kappa_{i0} T_i^{2.5} \Theta^2}$$

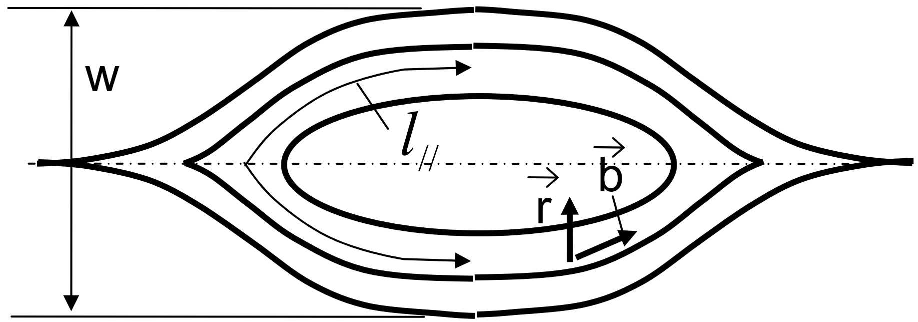

$$\Theta = \vec{b}\cdot\vec{r} \approx \frac{w}{l_{//}}$$

With high density & small Θ (~10^{-4} in LHD), $\dfrac{n\chi_\perp}{\kappa_{i0} T_i^{2.5}} >> \Theta^2$ **(Y. Feng NF 46 2006)**

⊥-transport dominates

$$\boxed{\nabla_{//} T_i \approx -\frac{q_r \Theta}{n\chi_\perp} \propto n^{-1}}$$

Increasing density suppresses //-T gradient, i.e. thermal force in the presence of remnant islands.

M. Kobayashi et al., Proceedings of 22nd IAEA FEC (2008) EX/9-4.

Radial profiles of each charge states of carbon density

Impurity screening → shift of impurity density profile to low temperature region

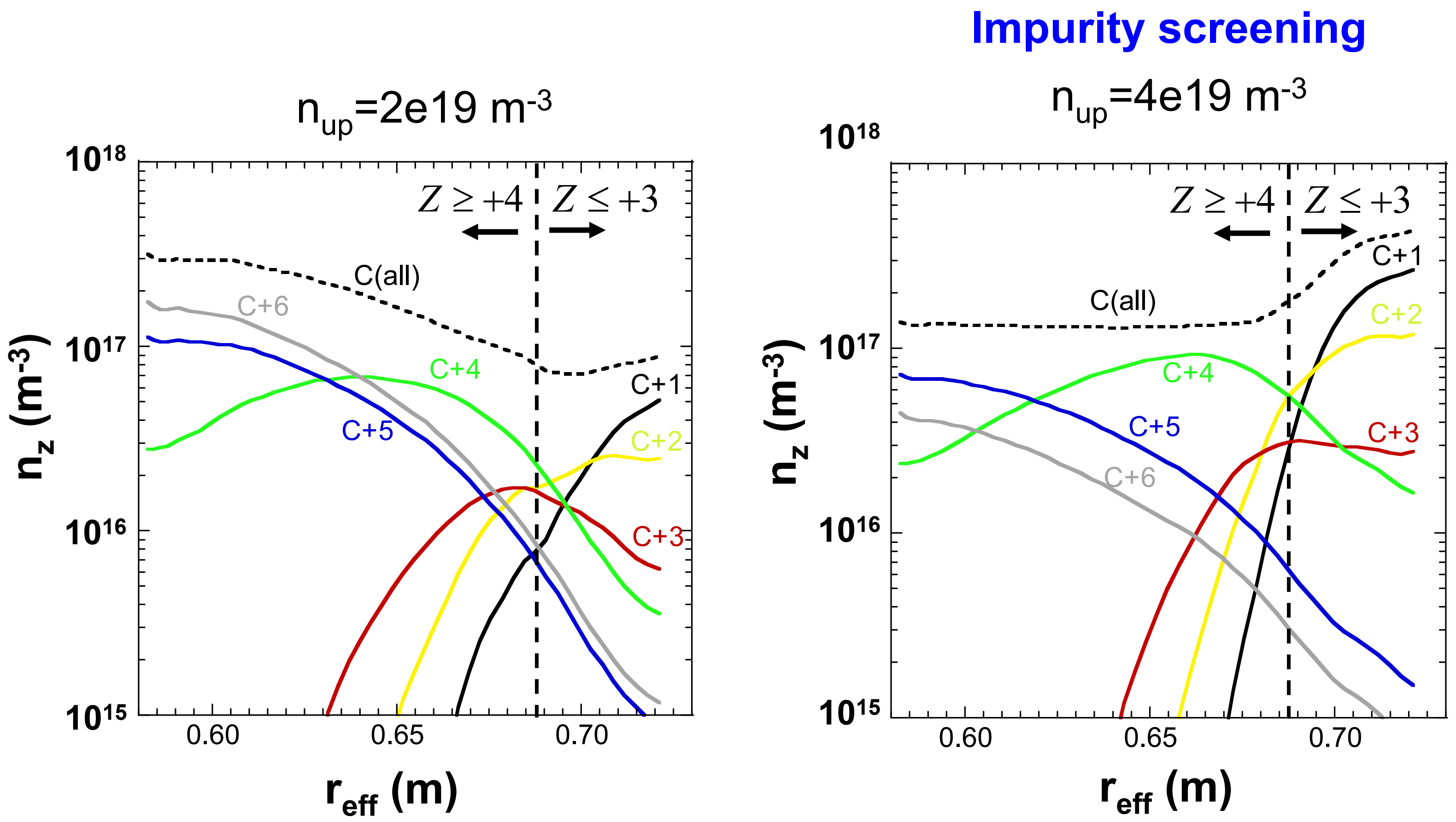

Emission measurements in experiments indicate impurity retention potential at high density

CIII: 977Å, $1S^2 2S^2$-$1S^2 2S2P$ (VUV monochromators)

CIV: 1548Å, $1S^2 2S$-$1S^2 2P$ (VUV monochromators)

CV: 40.27Å, $1S^2$-$1S2P$ (EUV spectrometer)

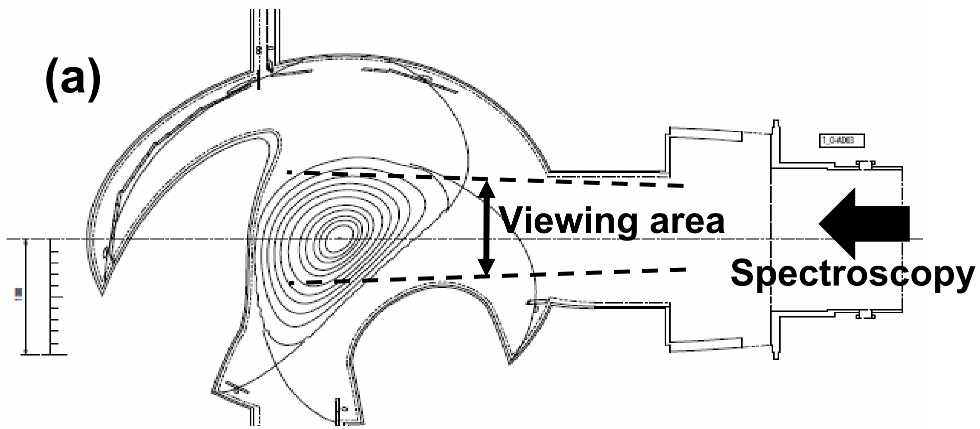

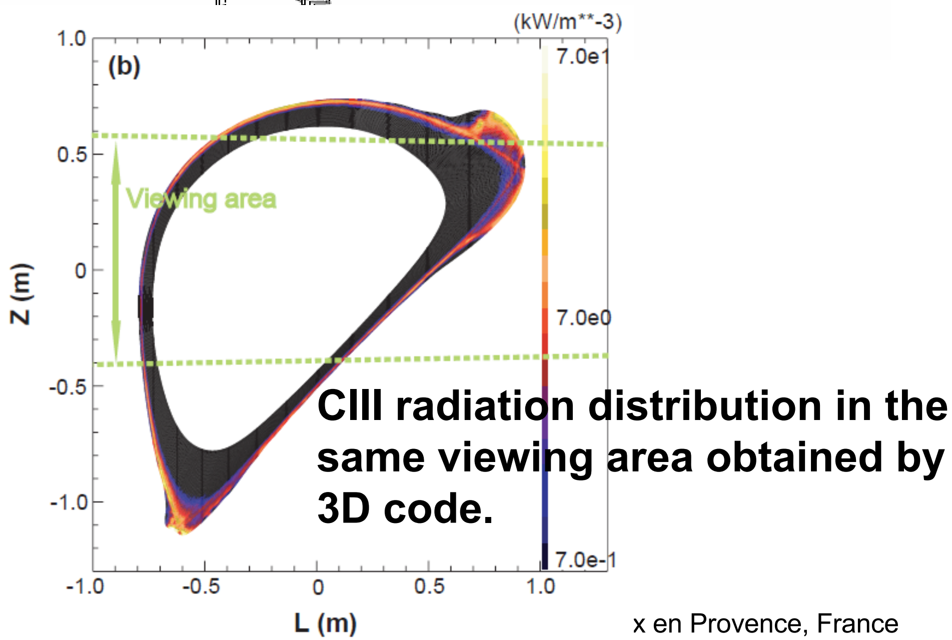

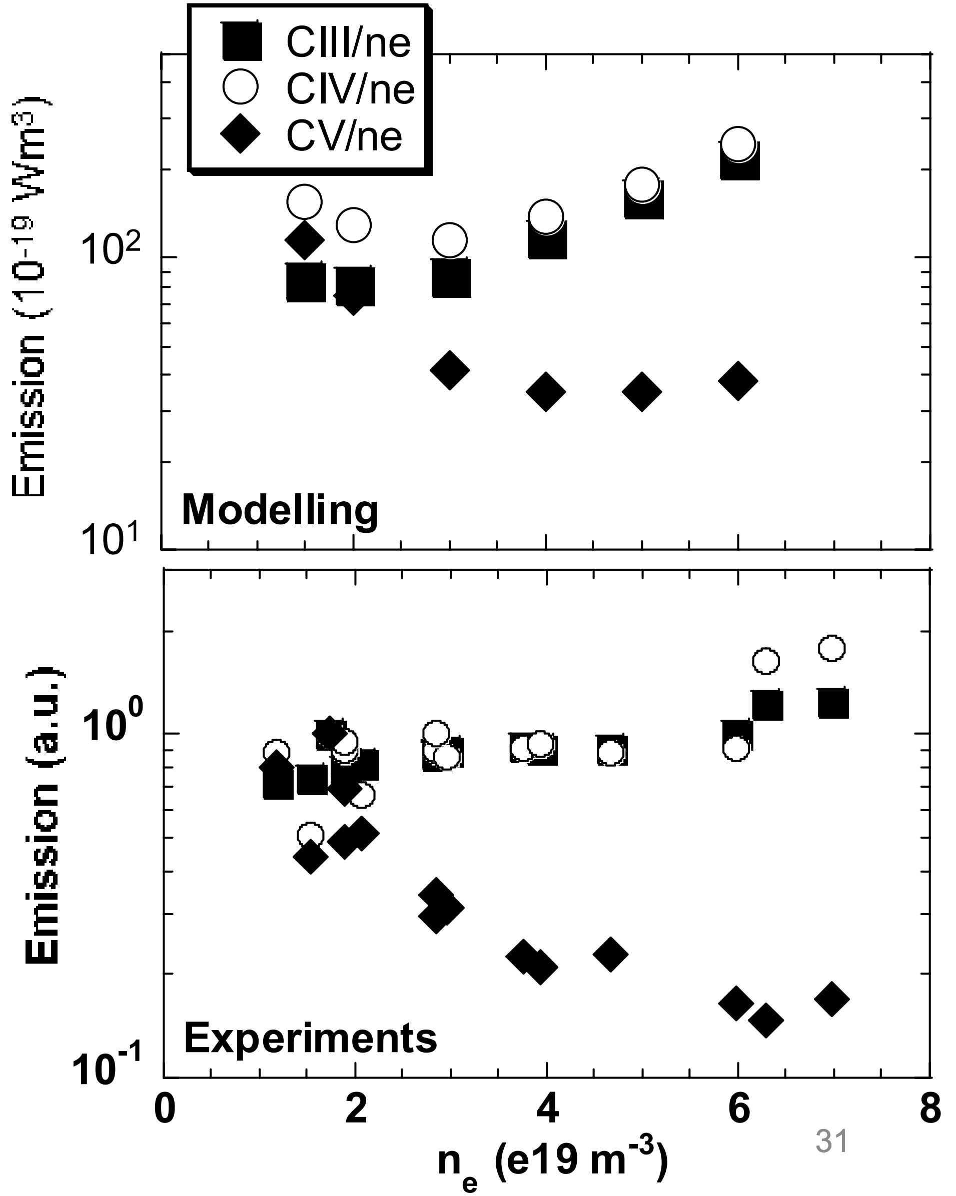

Signature of impurity screening with stochastic boundary various devices

Tore Supra Y. Corre et al., NF **47** (2007) 119.

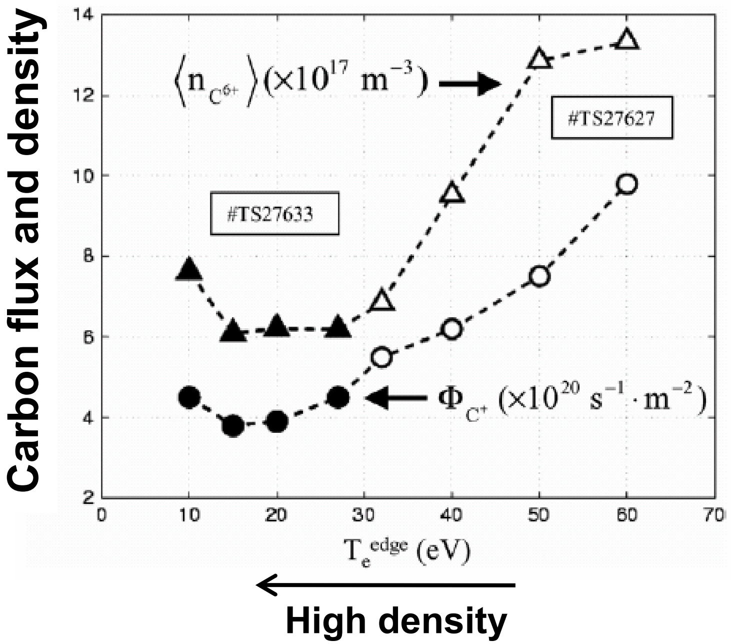

C^{6+} density in confinement region decreases with increasing density.

TEXTOR-DED G. Telesca et al., JNM **390-391** (2009) 227.

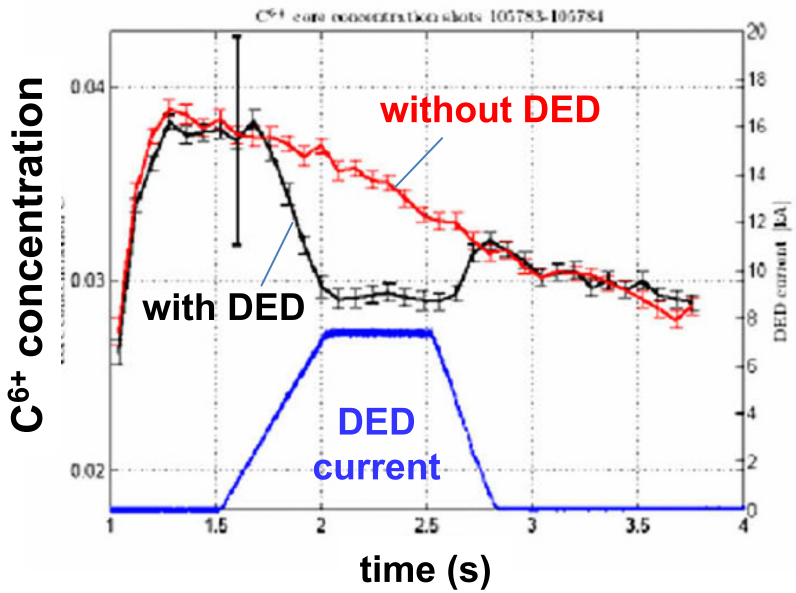

C^{6+} concentration in core region decreases with DED activation.

Summary: SOL Impurity transport

1. 3D impurity transport modelling in the stochastic magnetic structure shows impurity screening effect at high density :

   Increasing density

   ➔ Enhances friction force in edge surface layer with flow acceleration by rich ionization source

   ➔ Stops carbon penetration in edge surface layers ➔ Feels more friction

   ➔ Suppresses thermal force in stochastic region

2. The remnant islands with small $\Theta\,(\approx w/l_{//})$, $\dfrac{n\chi_{\perp}}{\kappa_{i0}T_i^{2.5}} >> \Theta^2$ and high density → $\boxed{\nabla_{//}T \propto n^{-1}}$

   i.e. suppression of thermal force at high density

3. The edge carbon emission measurements agree well with the code results, indicating impurity retention effect of stochastic magnetic boundary.

Summary

Plasma transport in stochastic magnetic boundary in LHD is analyzed by the 3D edge transport code in comparison with experimental results and with other devices.

1. Magnetic shear + RMP
   → topological change of field lines (magnetic island), stochastic instability
   → $\perp$, // characteristic scale: δ_m, w, $l_{//}$

2. Influence on divertor regime:
   high recycling ←→ no high recycling with $f_m \propto \dfrac{l_{//}}{T_d^{0.5}\,\delta_m^{\;2}}$

3. Impurity screening potential at high density with very small $\Theta\,(\approx w / l_{//})$, $\dfrac{n\chi_\perp}{\kappa_{i0} T_i^{2.5}} >> \Theta^2$ and flow acceleration in edge surface layers (laminar region).

These geometrical parameters provide control of edge plasma transport in stochastic SOL.

Stochastic magnetic boundaries
→Symmetry breaking
→ Controllability of edge plasma transport

<u>Further topics to be investigated</u>
Power load dispersal on divertor plates
Plasma response to RMP.
Electric field formation, determination of D,D_Z, χ.
Quantitative estimation for future devices

Field lines connect divertor plate with different connection lengths (ranges in two orders, 10 m ~ 1000 m)

➢Magnetic shear + $\tilde{B}_r$ → stretching, bending, compression of flux tubes

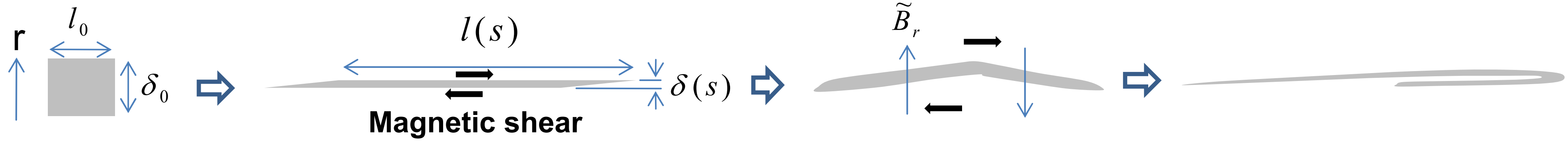

The long & short flux tubes are mixed due to the deformation, creating fine structure.

Not only //, BUT ⊥ energy exchange between flux tubes plays important role in determining wetted area.

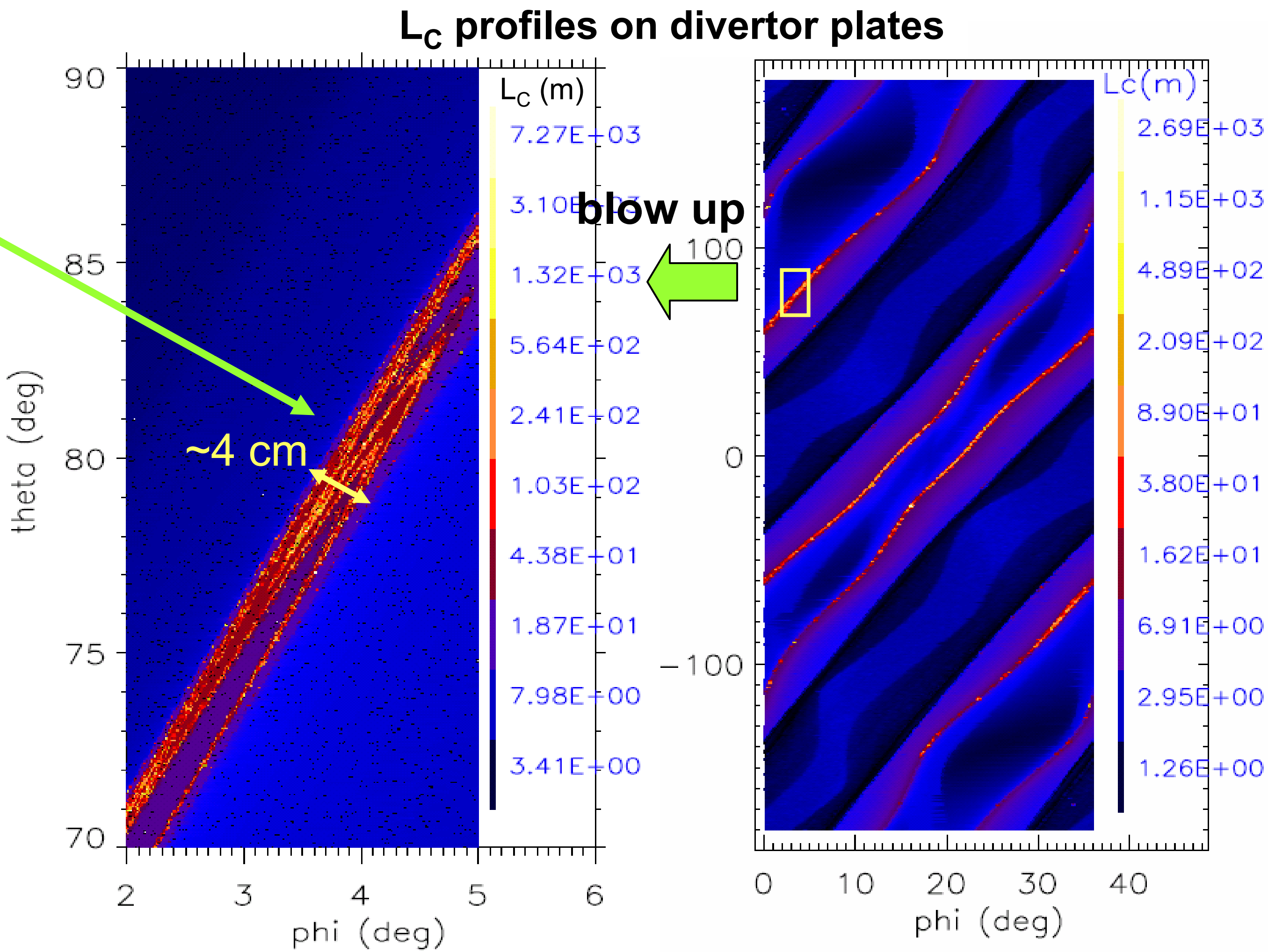

3D Modelling : Power deposition profile insensitive to P_{SOL}

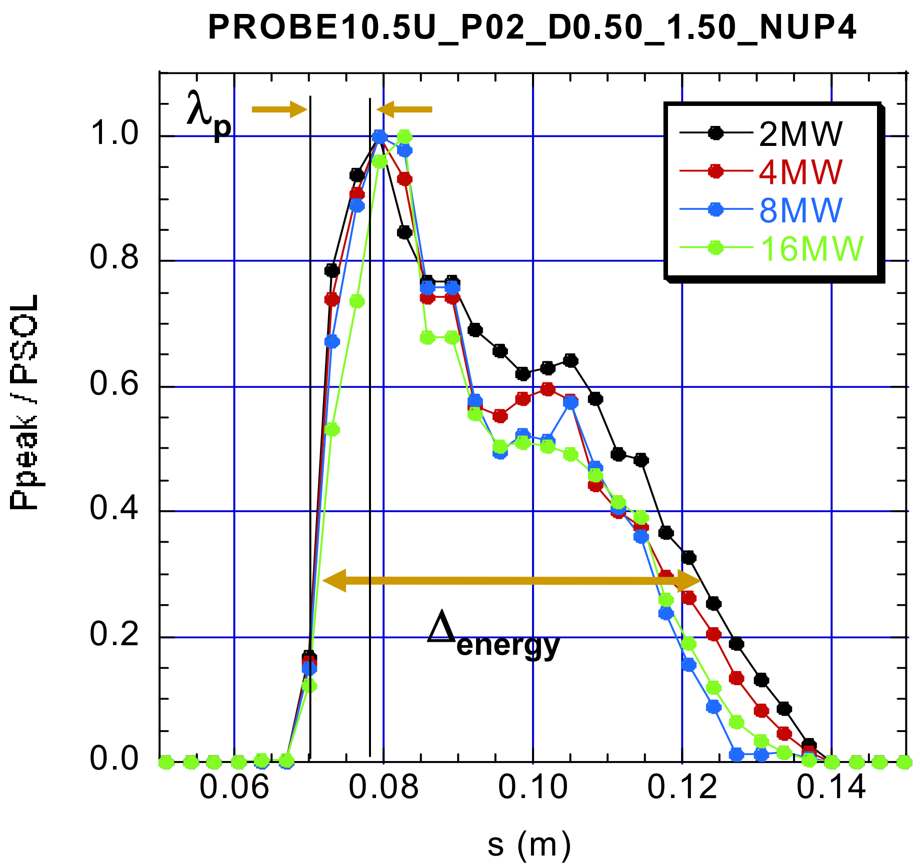

Maximum power load linearly scales with P_{SOL}, indicating no P_{SOL} dependence of Δ_{energy}.

Because of $\Delta_{energy} >> \lambda_p$, change of λ_p is negligible.

IR camera measurements in TEXTOR-DED: Divertor heat flux is well correlated with L_C distribution

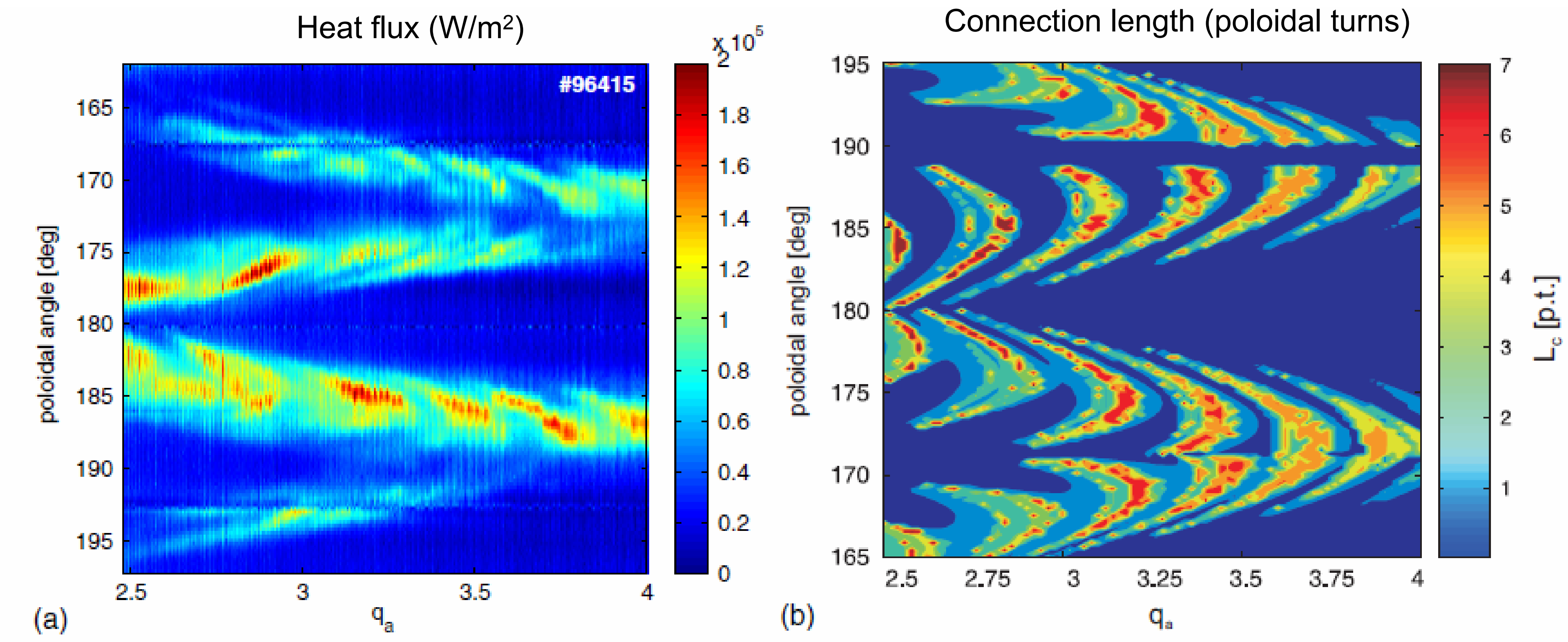

M. Jakubowski et al., PPCF **49** (2007) S109.

Plasma response to RMP : screening/amplification by current induced around resonance surface

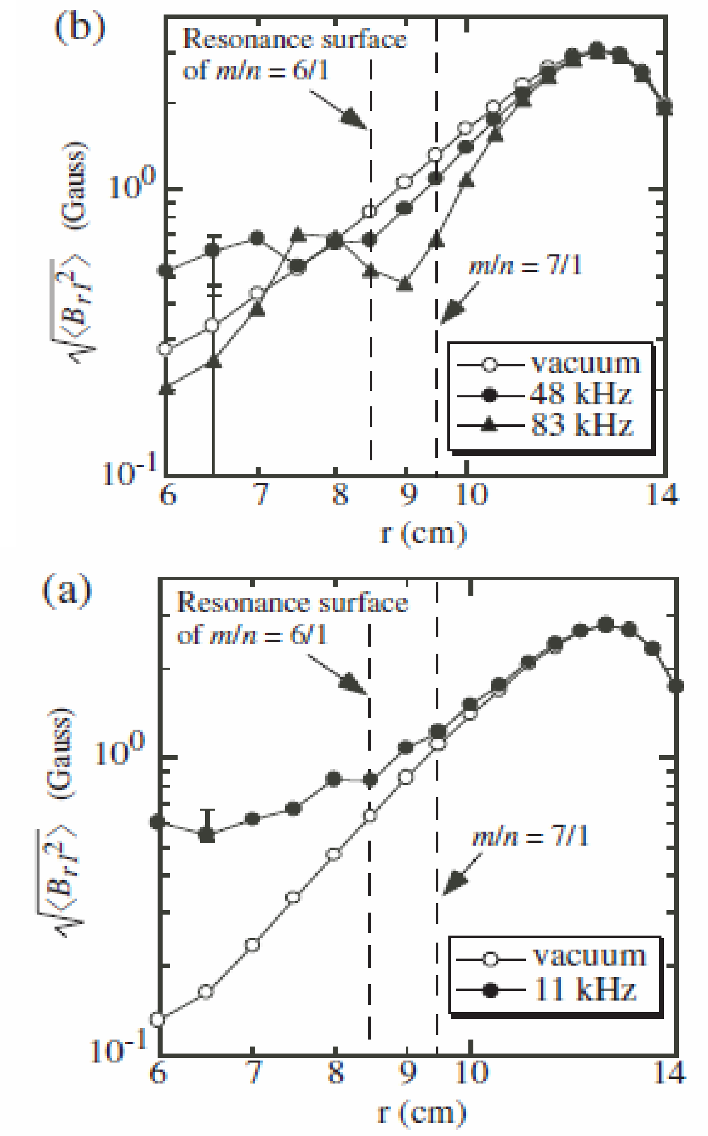

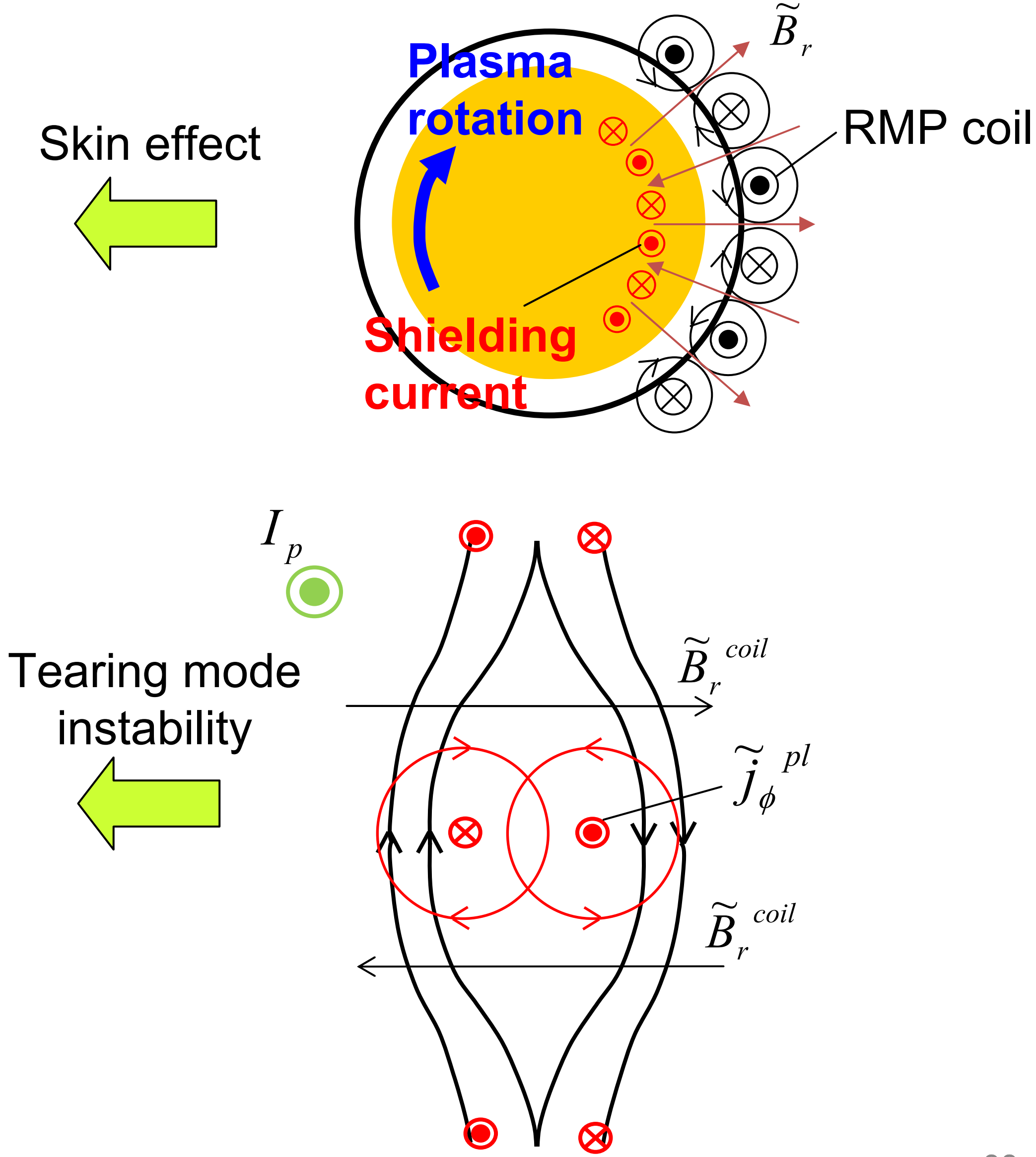

Y. Kikuchi et al. NF 44 (2004) S28.

Neo-classical effect : bootstrap current, polarization current

Island healing

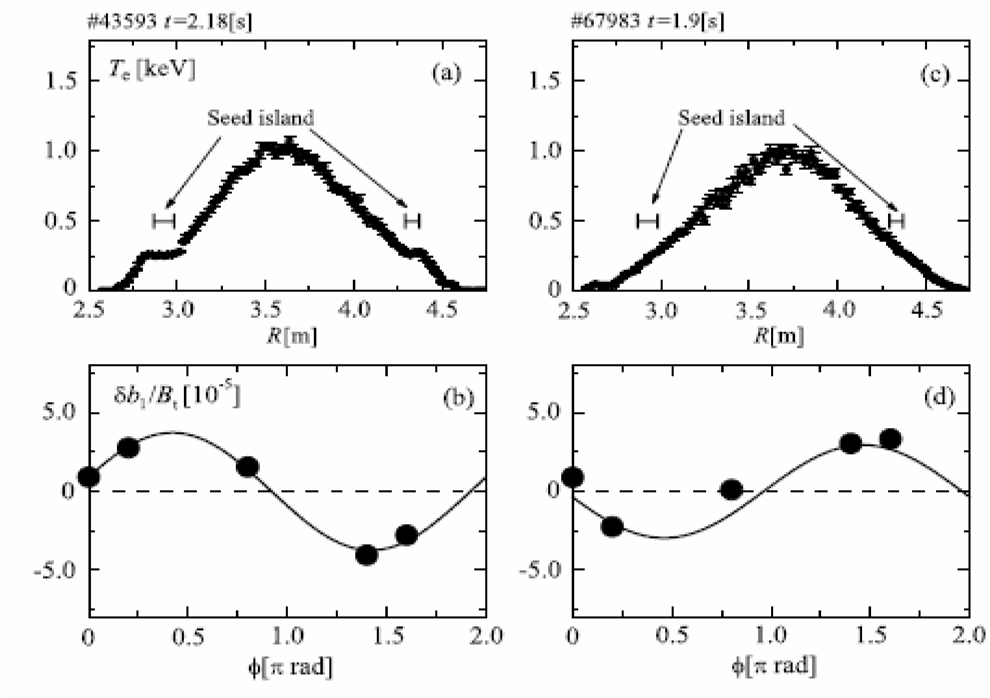

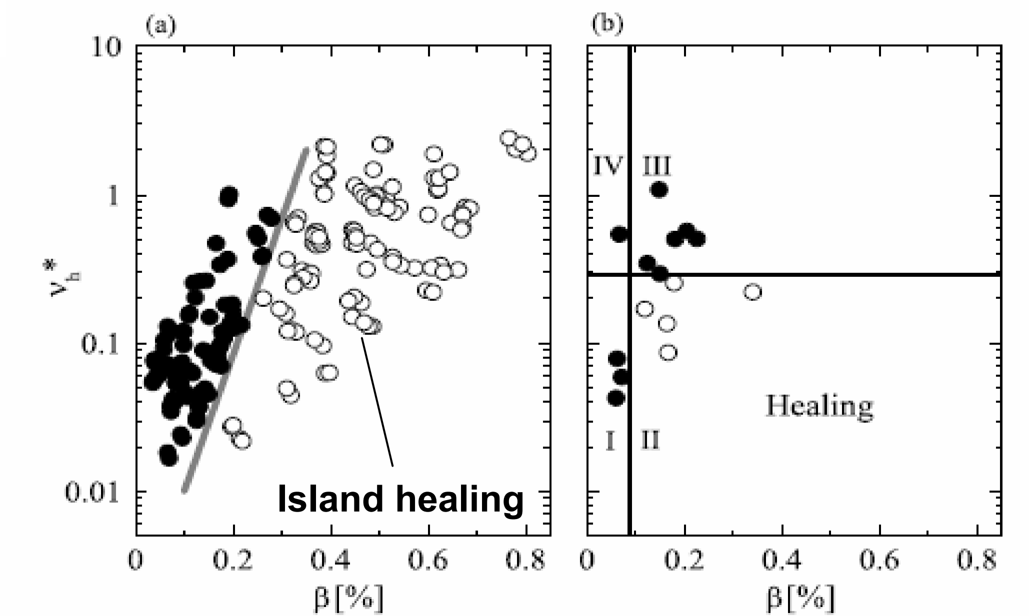

Figure 7. $\beta - \nu_h^*$ space. (*a*) Open circles indicate the cases where the island is not observed. Closed circles denote that the island is observed. (*b*) The $\beta - \nu_h^*$ space made from the acquired data in [3].

Y. Narushima et al., Nucl. Fusion **48** (2008) 075010.
N. Ohyabu et al., Phys. Rev. Lett. **88** (2002) 055005.
K. Itoh, S.I. Itoh and M. Yagi, Phys. Plasmas **12** (2005) 072512.

Possibility for stable detachment control with remnant island structure

Strong radiation is localized at the remnant island structure

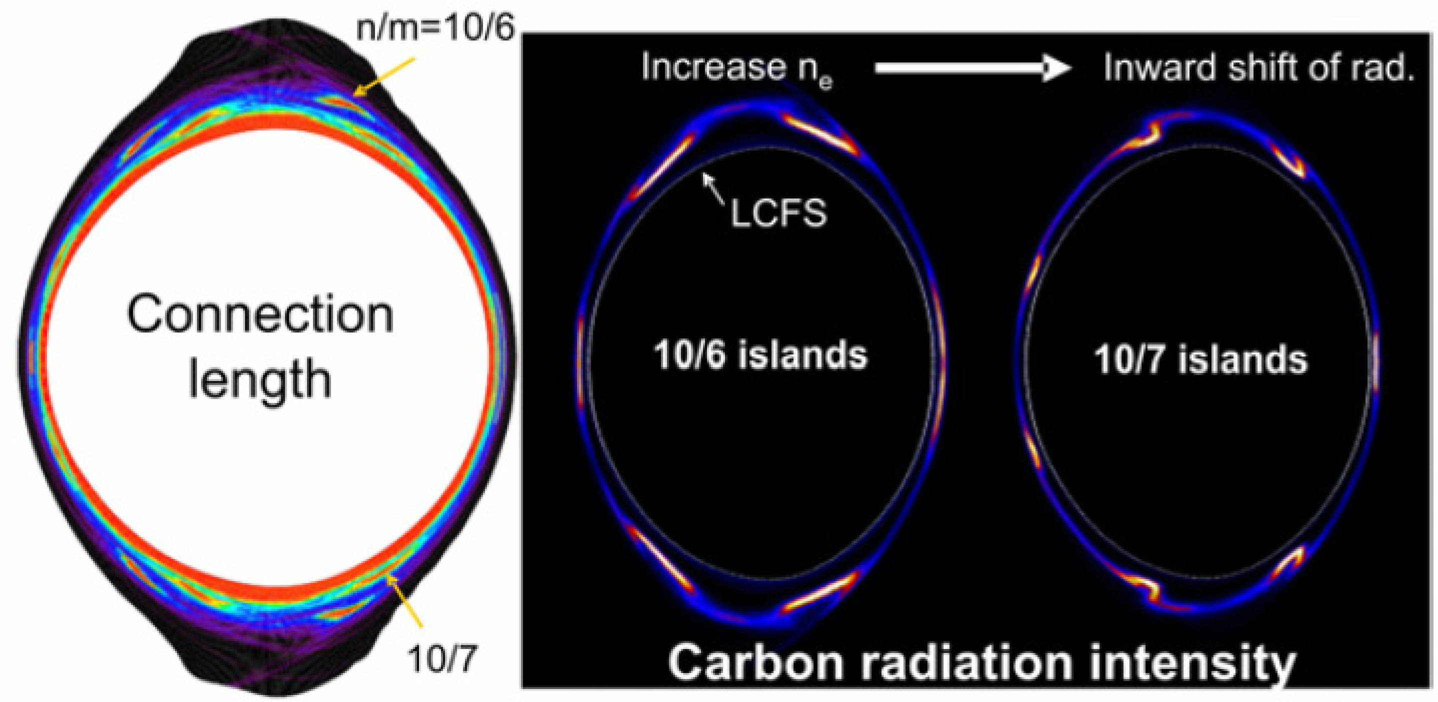

Y. Feng et al., NF **48** (2008) 024012.

Interaction of island chain of different modes at high field region leads to strong flow shear ➔ Momentum loss via cross-field friction

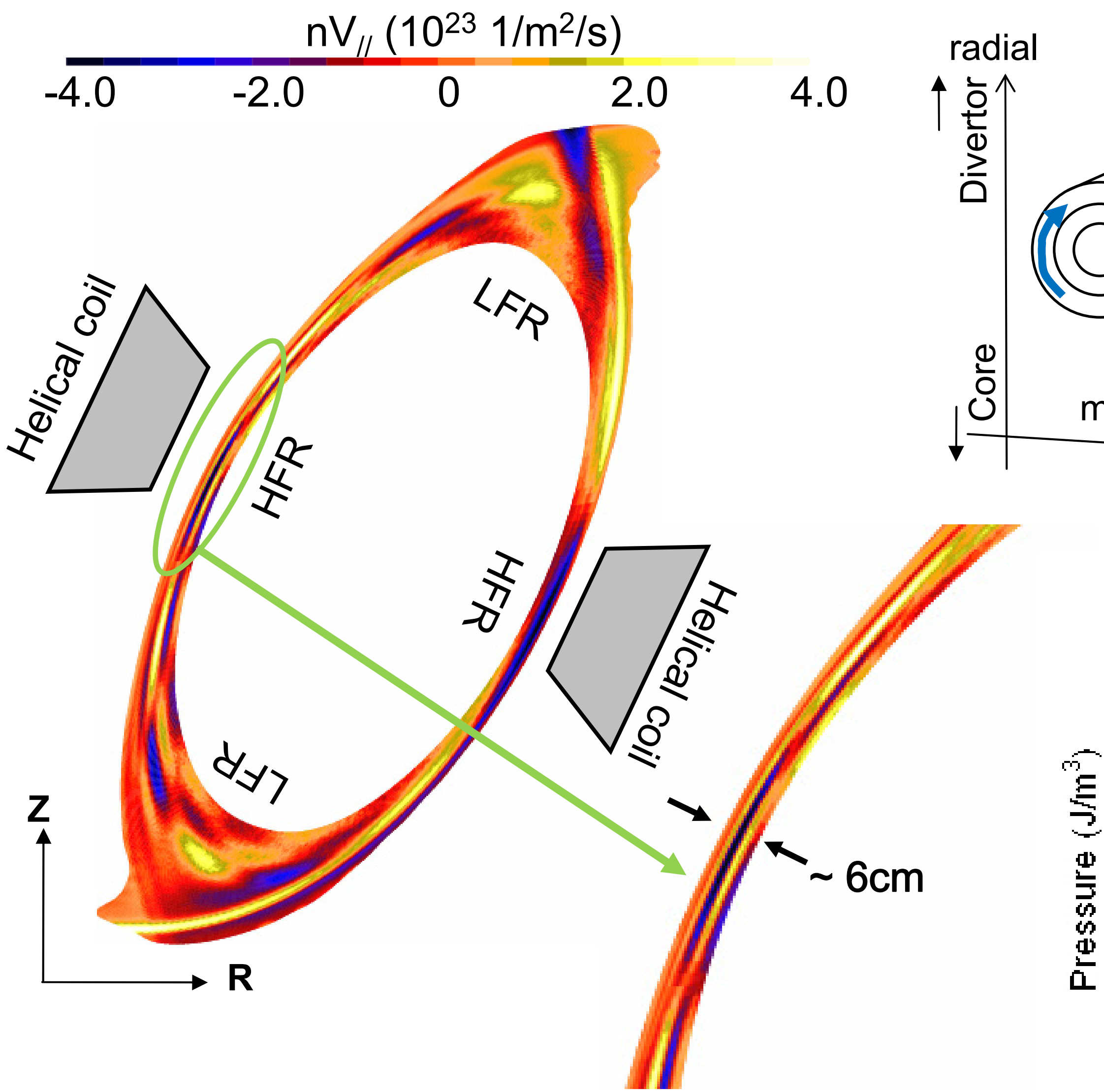

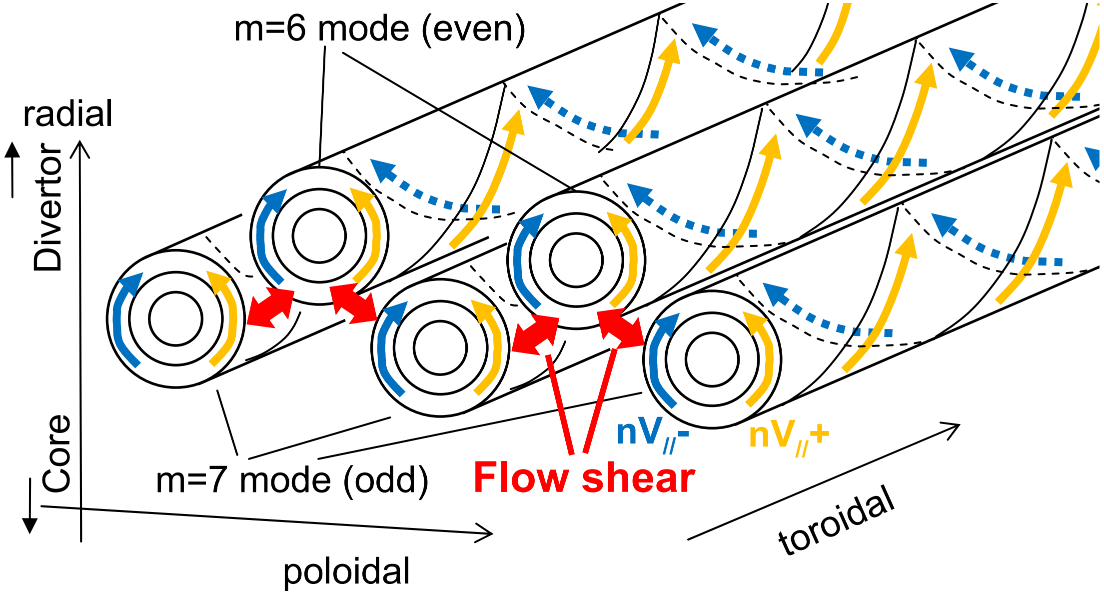

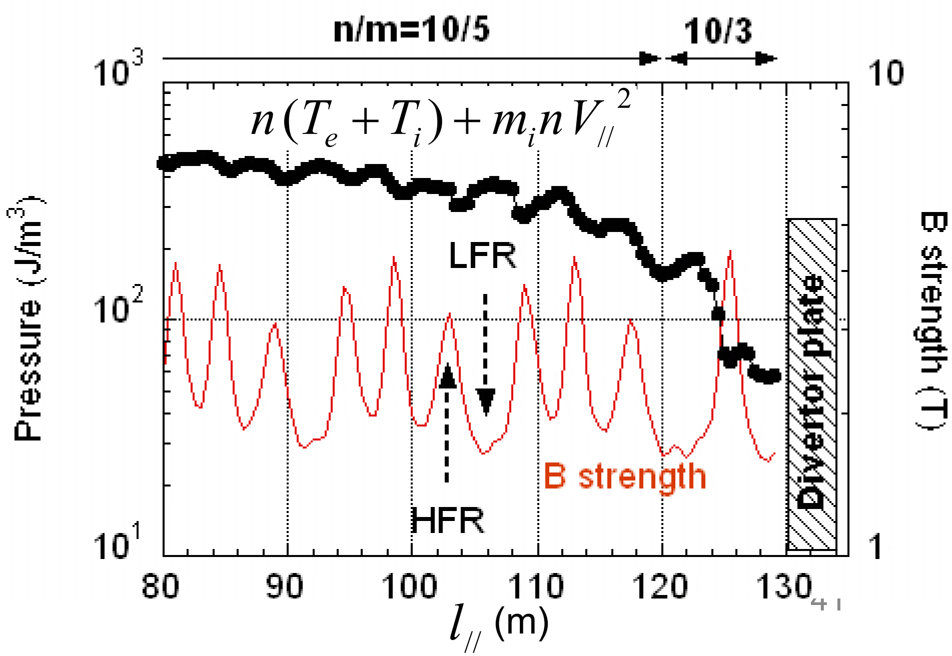

Parallel plasma flow is regulated by remnant island (mode) structure

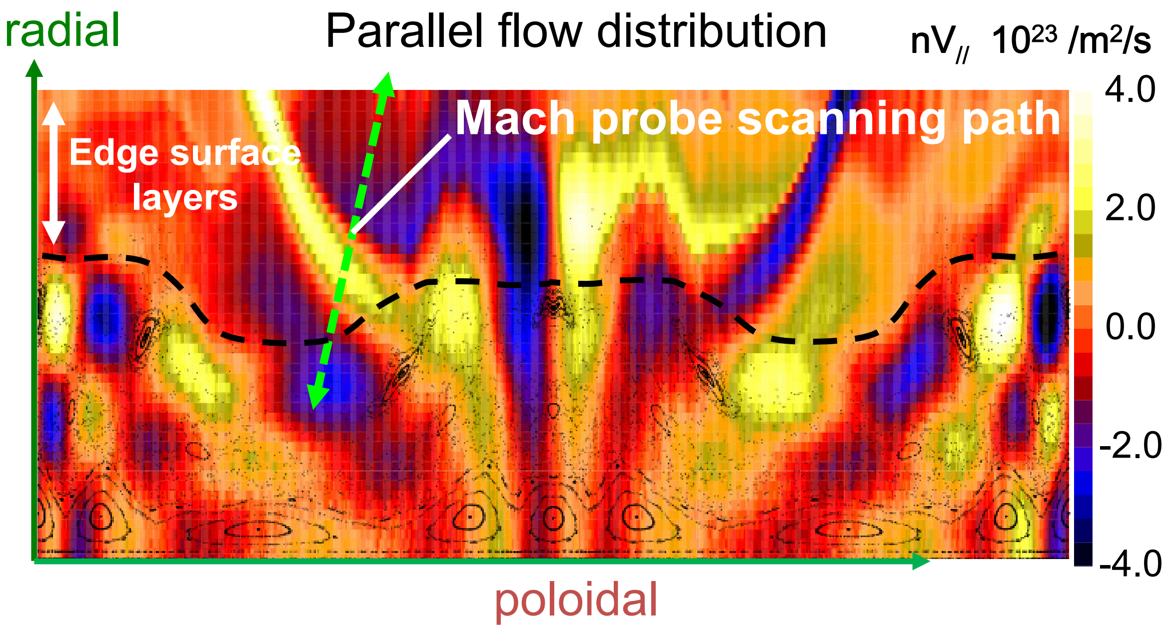

- The field line structure produces flow alternation.
- Short confinement time in open field lines leads to fast parallel flow, Mach>0.5
  → impact on impurity transport (discussed later)

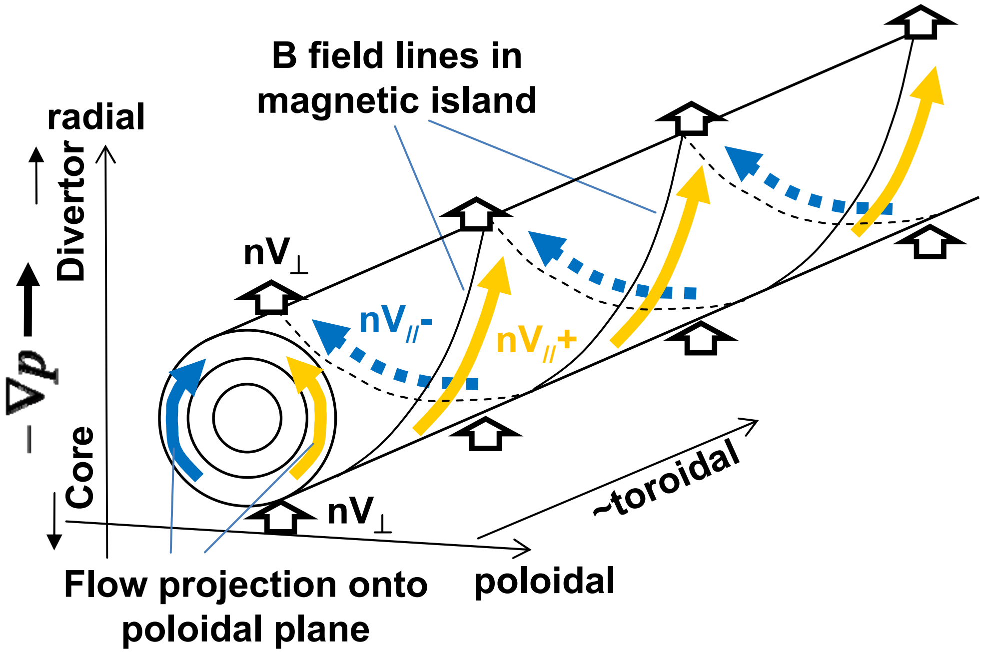

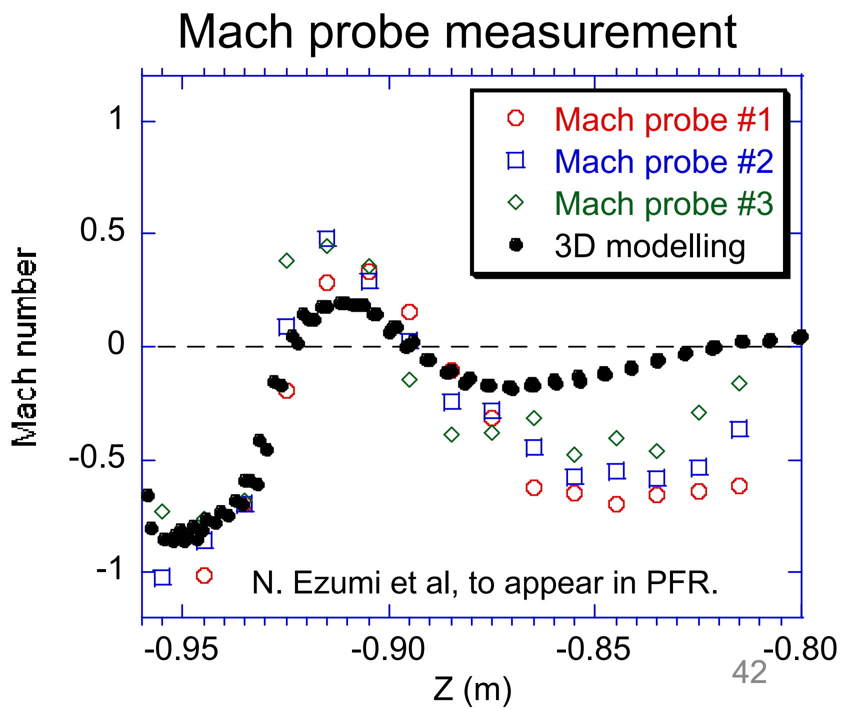

Parallel plasma flow is regulated by remnant island (mode) structure

Parallel flow distribution

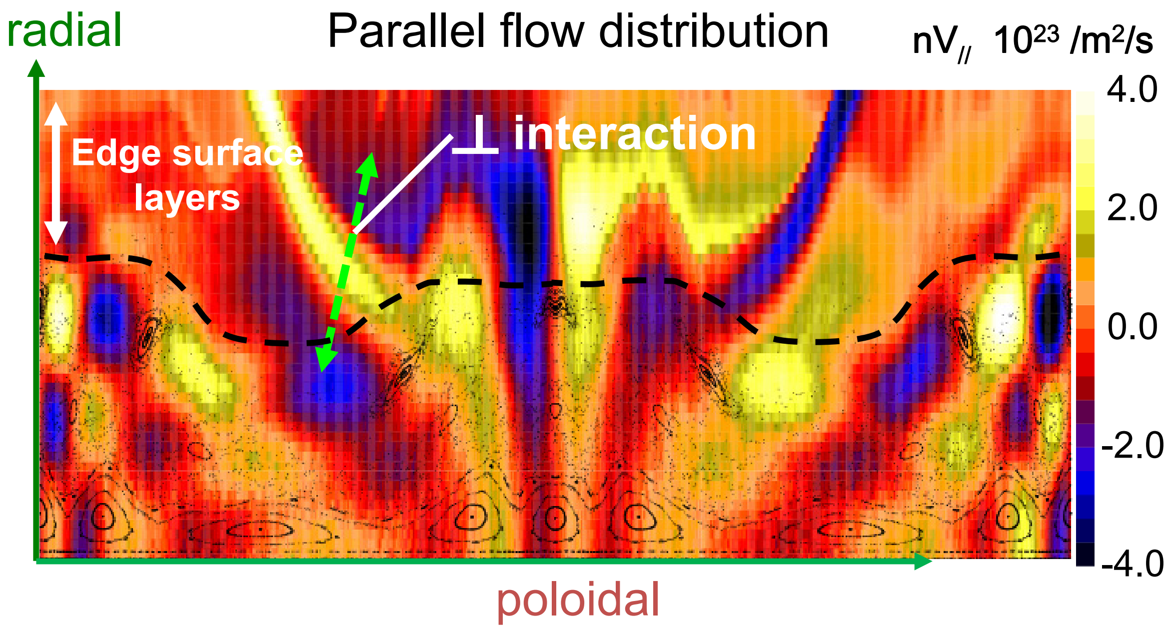

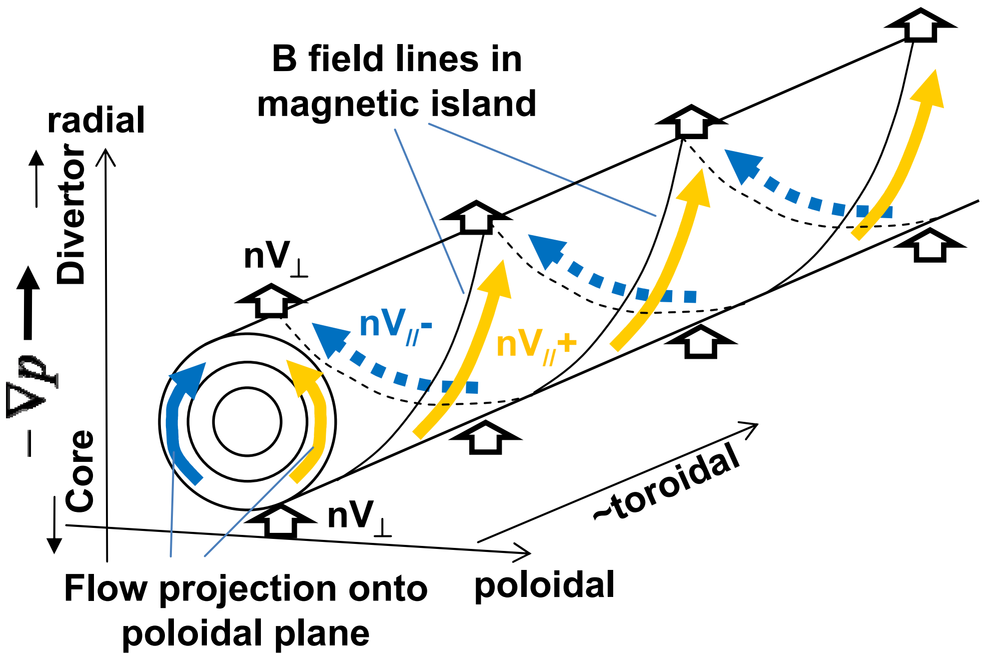

- ➢The flow shear → momentum loss of $V_{//}$ via $\perp$ interaction

$$\nabla_{\perp}(m_i V_{//} D_{\perp} \nabla_{\perp} n + \eta_{\perp} \nabla_{\perp} V_{//})$$

Mach probe measurement

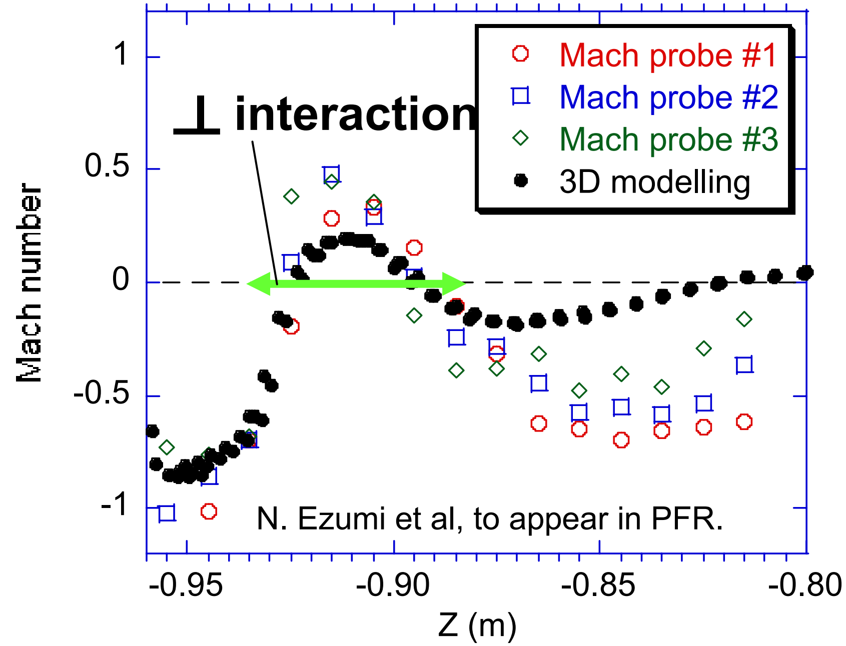

Summary of 3.1 Divertor plasma parameters

What we have learned

1. $nV_{//}$ in stochastic boundary → alternating flow regulated by remnant islands
2. n_{div} & T_{div} in stochastic boundary of LHD show modest sensitivity to n_{up}, in contrast to the high recycling regime in tokamaks.
3. Breakdown of parallel pressure conservation via perpendicular frictional interaction of the counter flows.
4. The degree of momentum loss can be described as $f_m \propto \dfrac{l_{//}}{T_d^{0.5}\,\delta_m^{\ 2}}$.
5. The analysis in W7-AS, X

   → controllability of divertor regime: $n_d \propto n_u^{\ 3} \leftrightarrow n_d \propto n_u^{\ 1\sim1.5}$
6. For future devices, $l_{//}, \delta_m$ should be optimized for control of divertor plasma.

   e.g. for good neutral compression, f_m should be small.

What we haven't yet understood

1. If D has parameter dependence, $f_m(n_d, T_d)$? → affects ***qualitative*** dependence!!
2. If $\perp$ momentum flux is not $\propto \nabla_{\perp} n V_{//}$, but convective one $\propto V_{\perp,conv} V_{//}$ then $f_m \propto \dfrac{l_{//}}{\delta_m}$?

   → affects ***quantitative*** dependence!

Summary: SOL Impurity transport

What we haven't yet understood

1. Parameter & Z dependence of $D_{Z\perp}$? → affects ***quantitative*** dependence!
2. $\perp$ convective term $\Theta V_{Z//} + V_{Z,conv}$? → affects ***qualitative*** dependence!!

Simplified // force balance between friction and ion thermal force reads,

$$V_{Z//} = V_{i//} + C_i \frac{\tau_{Zi}}{m_Z} Z^2 \nabla_{//} T_i$$

1D radial continuity,

$$\frac{d}{dr}\left(\Theta n_Z V_{Z//} - D_{Z\perp}\frac{dn_Z}{dr}\right) = -S_Z - R_Z + S_{Z-1} + R_{Z+1}$$

$$\sum_Z \rightarrow \frac{d}{dr}\left(\Theta n_I V_{Z//} - D_{Z\perp}\frac{dn_I}{dr}\right) = 0$$

Solution for target-released impurities:

$$n_{I,LCMS} / n_{I,target} = \exp\left(-\int_{LCMS}^{target} \frac{\Theta V_{Z//}}{D_{Z\perp}} dr\right)$$

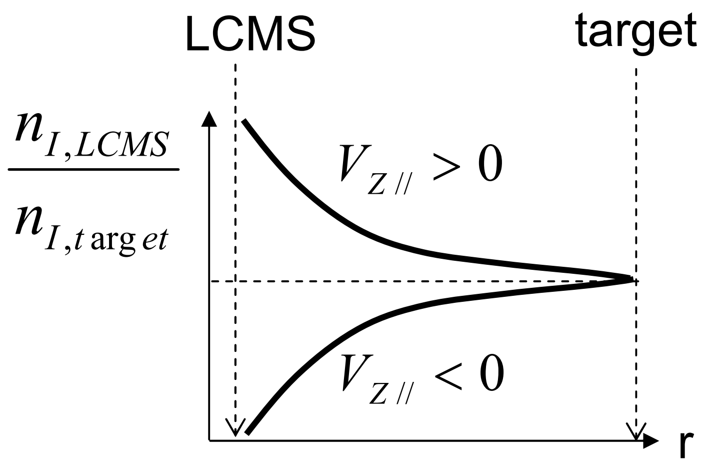

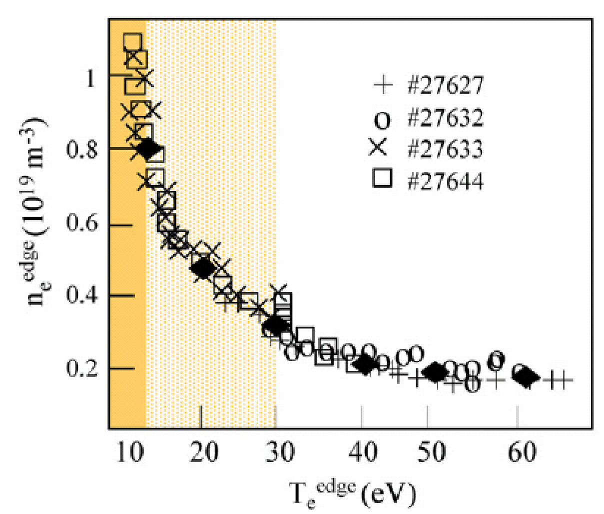

n_e^{edge} (10^{19} m^{-3})
1
0.8
0.6
0.4
0.2
10
20
30
40
50
60
T_e^{edge} (eV)
+ #27627
o #27632
× #27633
□ #27644

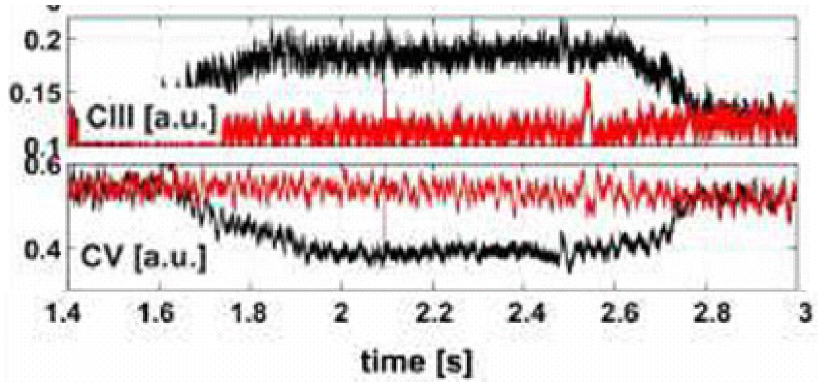

0.2
0.15
0.1
CIII [a.u.]
0.6
0.4
CV [a.u.]
1.4
1.6
1.8
2
2.2
2.4
2.6
2.8
3
time [s]

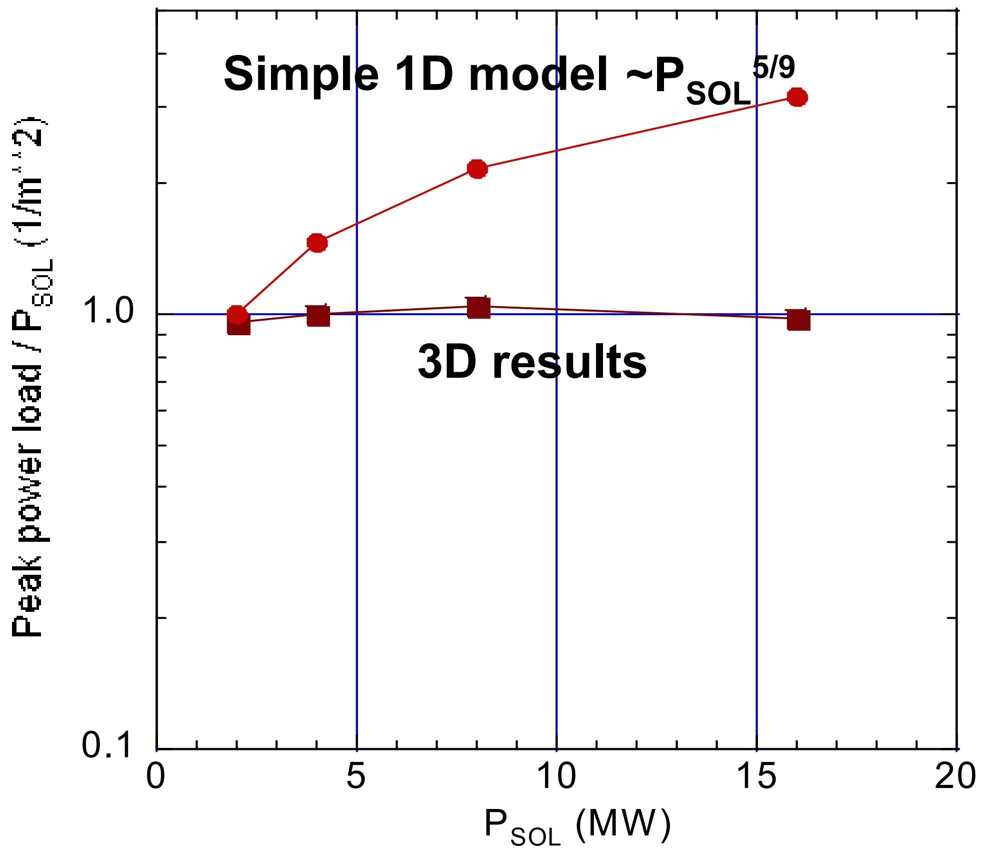
Simple 1D model ~P$_{SOL}$$^{5/9}$
3D results
Peak power load / P$_{SOL}$ (1/m``2)
1.0
0.1
0
5
10
15
20
P$_{SOL}$ (MW)